BARC
NEWSLETTER

BARC

राष्ट्र की सेवा में परमाणु
ATOMS IN THE SERVICE OF THE NATION

भाभा परमाणु अनुसंधान केंद्र
BHABHA ATOMIC RESEARCH CENTRE

IN THIS ISSUE

In the Forthcoming Issue

CONTENTS

From the Editor's Desk

At the outset I would like to thank all our colleagues for their enthusiastic response to the Founder's Day Special Issue 2013. We are happy to inform you that we received a total of 88 Award winning papers uploaded through our online portal. The publication process is in full swing.

We would like to remind you that through the channel of BARC Newsletter, information about ongoing R&D in BARC is disseminated both within BARC and outside to select national and international institutions. It is therefore necessary to make use of this platform and inform the scientific community about R&D progress and achievements in your field of expertise, be it through full length articles or through Brief Communications.

We are pleased to bring you the fourth issue of the BARC Newsletter published in this year. The issue carries five articles and two Brief Communications. R&D in Fusion technology is showcased through: one a full length article on solid breeder materials used in the Test Blanket Module (TBM) of the ITER and two a Brief Communication on characterization of Lithium Titanate using non destructive methodology for quantification of Lithium and Titanium. Another article describes the pioneering work on high average power aqueous dye lasers being carried out at BARC. A methodology for the modelling of the Critical Heat Flux phenomenon under BWR operating conditions is described in one of the articles.

Dr. K. Bhanumurthy
On behalf of the Editorial Committee

INDIGEL - A Material for Decontamination of Solid Surfaces

Nuclear Recycle Group

Decontamination of all structural surfaces used in processing/handling of nuclear materials is necessary either periodically or before dismantling. Radionuclide(s) in different chemical forms are held on the surfaces as loose or fixed contaminants. The diversity in nature of surfaces as well as contaminants demands case specific techniques for efficient decontamination leading to minimization of total man rem exposure and secondary waste. Among the various advanced techniques developed in recent years, the use of strippable gels is one of the attractive options for removal of radionuclide(s) from solid surfaces as it offers good decontamination performance and produces a low amount of secondary waste.

A strippable gel, INDIGEL, developed recently in our laboratory shows excellent capability for decontamination of radionuclides from surfaces like stainless steel, glass, granite, PVC floor, etc. The INDIGEL, an organic polymeric hydrogel, is prepared in viscosities ranging from 4-10 poise. Highly viscous (> 8 poise) gel is required for application on vertical surfaces and also on surfaces of complex geometry. Curing of the gel is complete within 16-24 hours under ambient conditions and then removed by peeling as a dry sheet. While curing, the contaminants are trapped in gel either physically or chemically depending upon the chemical state of the radionuclide(s). The INDIGEL is acidic and the spent gel is water soluble. These two properties make it unique among internationally known strippable gels.

During product evaluation trials, multiple surfaces were decontaminated utilizing INDIGEL with impressive results. Decontamination of a routinely used stainless steel fume hood, which was slightly corroded and had salt deposits, dust and red oxide powder is presented here as a standout example. About 1.5 Kg of wet gel was used to cover 3.4 M^2 area. The peeled gel weighed only 380 g. Excellent cleaning of the fume hood was obtained as evident below.

The first application of INDIGEL on actual alpha contaminated surfaces on a SS pump head and a glass door of fume hood showed complete reduction of alpha activity to below background level in a single application. Exploratory trials are underway to establish its effectiveness in decontamination applications.

After application

After peeling

Non-Destructive Compositional Characterization of Lithium Titanate (Li$_2$TiO$_3$) by Particle Induced Gamma-ray Emission and Neutron Activation Analysis

Radiochemistry and Isotope Group

Lithium based ceramics like Li_2O, Li_2ZrO_3, Li_2TiO_3, $LiAlO_2$ and Li_4SiO_4 are being widely studied as tritium breeding materials in D–T based fusion reactor under International Thermonuclear Experimental Reactor (ITER) programme. Due to good chemical stability and tritium recovery at low temperature, lithium titanate (Li_2TiO_3) is considered as one of the most suitable candidates. At Fuel Chemistry Division, BARC, Li_2TiO_3 was synthesized through sol-gel route. Lithium titanate microspheres (Fig. 1) were prepared by dispersing feed solution containing mixture of 3M HMTA, urea, 3M $TiOCl_2$ and 3M LiCl and/or $LiNO_3$ solution in the required ratio (Li:Ti = 2:1 mole ratio). For process optimization as well as chemical quality control it is necessary to quantify lithium and titanium contents, which is difficult by conventional wet chemical spectroscopic techniques.

An *in situ* current normalized Particle Induced Gamma-ray Emission (PIGE) method using proton beam at Folded Tandem Ion Accelerator (FOTIA), BARC was standardized for non-destructive quantification of Li in Li_2TiO_3. The element F was used as *in situ* current normalizing standard. PIGE, which is a powerful isotope specific nuclear analytical tool for the quantification of low Z elements like Li, Be, B, C,N.O, F, Na, Mg, Al and Si, involves measurements of prompt gamma-rays from proton induced nuclear reactions. A PIGE facility has been set up at FOTIA by Radiochemistry Division (Fig. 2). Sample and standard pellets, prepared in cellulose matrix along with fixed amount of F (in the form of CaF_2) were irradiated with 4 MeV proton beam at ~10 nA current. Gamma ray yields of ^7Li and ^{19}F at 4 MeV proton beam are given in Table 1. Lithium contents in the range of 43-44.7 wt% were quantified by relative method by measuring prompt γ-rays of 429 and 478 keV from ^7Li (p, nγ) ^7Be and ^7Li (p, p'γ) ^7Li reactions using high resolution gamma-ray spectrometry (Fig. 3). Instrumental Neutron Activation Analysis (INAA) was used for Ti determination in Li_2TiO_3 by indexing 320 keV γ-ray from ^{50}Ti (n,γ) ^{51}Ti reaction using high neutron flux at Pneumatic Carrier Facility (PCF) of Dhruva reactor. Li/Ti mole ratios obtained were found to be in good agreement with that of stoichiometric Li_2TiO_3, indicating optimization of synthesis procedure. PIGE method is also suitable for simultaneous quantification of Li and Si in Li_4SiO_4 and Li and Al in $LiAlO_2$. Due to isotope specific nature, PIGE is capable of quantifying isotopic composition of Li (i.e., ^6Li and ^7Li) simultaneously using ~1.8 MeV proton beam. Thus a comprehensive non-destructive methodology has been optimized for quantification of Li and Ti contents in lithium titanate.

Table 1: PIGE reactions and γ-ray yields of ^7Li and ^{19}F

Element	Reaction	E$_\gamma$ (keV)	Yield (Counts /µC-sr)
Li	^{7}Li (p, p' γ) ^{7}Li	478	8.1x10^7
	^{7}Li (p, n γ) ^{7}Be	429	2.6x10^7
F	^{19}F (p, p' γ) ^{19}F	110	~1.1´10^7
	^{19}F (p, p' γ) ^{19}F	197	4.3´10^7

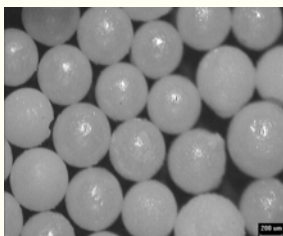
Fig. 1: Optical photograph of sintered Li$_2$TiO$_3$ pebbles

Fig. 2: PIGE set up at FOTIA: Beam chamber and HPGe detector
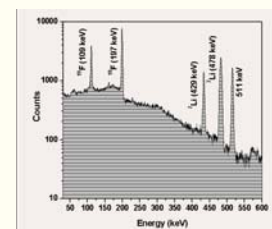

Fig. 3: Gamma ray spectrum of Li$_2$TiO$_3$ with CaF$_2$ in PIGE using 4 MeV proton beam

Dr. S. Kailas, Former Director, Physics Group, BARC in conversation with members of the BARC Newsletter Editorial Committee

1. **Physics Group one of the oldest groups,was formed by Dr. Homi Jehangir Bhabha, founder of BARC. How far have we met the expectations of our Founder?**

Right from inception of the DAE, Physics discipline has occupied a pride of place in the growth of the atomic energy programme of the country. The Physics Group (PG) has had a rich scientific lineage and some of the Directors of the group went on to become Director of BARC and also Chairman of the DAE. Over the years, PG has contributed significantly to various R & D programmes of BARC which were also of great relevance to DAE. The primary mandate of PG continues to be the pursuit of excellence in frontier areas of physical sciences. In addition, PG is involved in activities that include: indigenous development of instrumentation, operation of national facilities, playing a lead role in several mega science programmes both at national and international levels and involvement in educational programmes at the Homi Bhabha National Institute and at the DAE-Mumbai University Centre of Excellence in Basic Sciences.

2. **India has launched a few mega science projects such as Accelerator Driven sub-critical System (ADS),** *Major Atmospheric Cerenkov Experiment (*MACE) **and Indian Neutrino Observatory (INO). Do we have adequate trained man power to execute these projects?**

Science interest is the key driver in mega science programmes like INO and MACE. As it happens in many of the programmes of this nature, even though the PG is the initiator, entire BARC participates in the activity. Both INO and MACE are world class facilities. The ADS is a DAE programme and PG is making important contributions, in particular, in the development of the accelerator. We collaborate with other DAE units in executing

mega science projects.We do interact and consult with our international peers. While at the project initiation stage a smaller manpower is sufficient, at a later stage dedicated scientists, engineers, technical people would be required for installation, commissioning, operation and utilization.

3. **Particle accelerators have applications in many fields of science and also in industry. What is the roadmap for Particle Accelerators in India?**

Accelerators were originally developed for research in nuclear and particle physics. Now the utilization of accelerators has gone much beyond pure R&D. According to a survey, the total number of accelerators, big and small, electron and ion types is nearly 30,000. A large percentage isused for industrial purposes. In India, the number of accelerators is less than 100. In the next 20 years, I would expect this number to be multiplied several times. The DAE has an active programme for indigenous development of ion and electron accelerators for various applications. Development of Electron accelerators for cargo scanning is an important activity of BARC. Ion accelerators, both continuous and pulsed, with energies close to 1000 MeV are being developed. The Spallation Neutron Source (SNS) is coming up at the Raja Ramanna Centre for Advanced Technology. BARC is developing a high-energy high-intensity proton accelerator as a part of the Indian Accelerator Driven subcritical System (ADS) programme. A hadron therapy machine for cancer treatment is being planned by the Tata Memorial Hospital. The work on the development of national Radioactive Ion Beam(RIB) facility has been taken up by the Variable Energy Cyclotron Centre. The Saha Institute for Nuclear Physics is taking steps towards the development of the next generation synchrotron source. Fast neutron-based explosive detection is another development and this is an area of current interest for national security. BARC has an active programme in this area. DAE is also collaborating with Fermi Lab for the development of high energy

and high intensity proton accelerator which will expedite our indigenous efforts.

4. What is the importance of the MACE project?

MACE telescope is a state-of-the-art instrument with high sensitivity, for detecting very high energy gamma rays coming from active galactic sources. It is a 21 metre diameter telescope, which will be located at a height of 4200 meters at Hanle, Jammu and Kashmir. It will have a detection sensitivity of 30 GeV to 5 TeV for high energy gammas. The facility is expected to be installed and made operational at Hanle by the end of 2014. The set up will be fully assembled and tested at the Electronics Corporation of India Limited by the end of this year. MACE will also help in bridging the gap between land-based and satellite-based observations in terms of energy limits. It will be the main instrument in the northern sky. A similar one is already operational at Namibia (HESS) in the southern hemisphere.

5. Nuclear wastes, particularly High Level Wastes contain very long-lived actinides and fission products. What steps are being taken by the Physics Group to tackle this issue?

The DAE has been following the closed fuel cycle for our nuclear programme. This has resulted in generation of lesser amount of nuclear wastes. We also have programmes for separation and partitioning of minor actinides and fission products for various applications. All these efforts will further reduce the quantity of long-lived wastes either for transmutation or for ultimate storage and disposal. R & D towards nuclear waste incineration either in fast reactors or through ADS type facility (Accelerator Driven Transmutation) will have to be pursued vigorously.

6. How far have the National Labs in India been successful, in delivering benefits to the society? Please highlight some of the societal benefit programmes that are pursued by the Physics Group.

The benchmark of research and development is its utility to society. While the mandate of DAE is generation of safe, economical nuclear power in a sustained manner, it also has a large number of programmes, based on radiation and radiation-related technologies for the benefit of the society (radioisotopes for water, health care, agriculture, food and industry). Some of the R & D programmes of PG are driven by the requirements of nuclear power programmes in general. The R & D programmes of PG generate spin offs which are of interest to society. Specifically, PG has developed a medical imaging (filmless) setup and has transferred this knowhow to industry. As a result of intense research on magnetic materials, PG has come up with nanomaterials which can be used in healthcare. PG has also developed mass spectrometers, sensorsand detectors etc., for societal benefit. Operation of national research facilities by PG for university users is another societal activity of great significance. The ongoing R&D activities related to ADS, solar cells, accelerator technology, radiography/tomography, sensorsetc. will ultimately benefit society.

7. Can you tell us about the national facilities that are operated by the Physics Group?

The PG has been operating a number of major national facilities: The Pelletron with Super Conducting LINAC(joint facility of BARC-TIFR), FOTIA and PURNIMA fast neutron facilities at Trombay, the National Neutron Beam Facility at Dhruva (in association with the UGC), the TACTIC telescope at Mt. Abu, state of the art facilities for investigation of matter under both static and dynamic pressures and several beam lines (EXAFS, ARPES, EDXRD, HRVUV, Protein crystallography, photo-physics) at INDUS, RRCAT. Some more beam lines – PASS, IRFTS, SAXS and Imaging- are at an advanced stage of completion and they will be made available to the user community shortly. These world-class facilities will further enhance R&D in frontier areas of Physical Sciences.

8. Physics Group has several indigenous technology development programmes like mass spectrometers and detectors. Can you highlight the achievements in the topics?

The indigenous development of instrumentation is a strong and continuing activity of PG. Nearly 25 high precision mass spectrometers of different types have been developed and supplied to DAE users. Silicon detectors, Laser materials, gas sensors, crystals of different kinds and He-3 and BF3 detectors have been indigenously developed and supplied for various programmes.

Development of 10 mt long periscope for FBR programme, setting up of multilayer coating facilities, catalytic recombiner cards for NPCIL, bottle double decapper gadget for A3F,KARP, X-ray and neutron based imaging for DAE programmes, RPC detectors for CERN programme are some of the indigenous activities driven by PG.Trace analysis of nuclear and detector grade materials and development of associated instrumentation for various users are other important activities of the PG.

9. It is generally felt that there is a wide gap between the National Laboratories and Universities in India. How can we reduce this?

There is a gap between the national labs and the universities which needs to be reduced. This is due to non-availability of advanced research facilities for students. The issue is being addressed through joint BRNS programmes involving DAE and several educational institutions, and including them as partners in collaborative research through MoUs. We are also funding conferences, organizing conferences, hosting students during summer and visiting universities to give lectures. The DST Programme "Fund for Improvement of S&T Infrastructure in Higher Educational Institutions" (FIST) is one such initiative for advanced research. Several Senior DAE colleagues are more actively involved in teaching. All these efforts will help

strengthen the cooperation between DAE and educational institutions in the long run. We need to nurtureuniversities, the ones which traditionally provide manpower in the form of bright students to DAE.

10. Can you brief us about the various national/international collaborative programmes undertaken by Physics Group?

The PG has active international collaborations of great relevance to DAE programmes.We have successful ongoing collaborations with CERN, GANIL(France), ILL(France), FAIR(Germany) and Fermi Lab. We have an MoU with Belgium on the MYRRHA- ADS demonstrator project. At the nationallevel,we are collaborating with DAE units like IGCAR, IPR, RRCAT and VECC.In addition, we collaborate with universities, through the DAE-UGC and BRNS mechanisms.

11.There is a feeling that "Velocity of Research" in India is small. In what way can we increase the "velocity of research" in the area of physical sciences (basic and applied) and catch up with the advanced countries?

In the year 2005, Dr. R. Chidambaram, PSA to Govt. of India had organized a theme meeting on the subject: "Attracting Young People to careers in Science". Three issues were addressed: Retention of talent; Improving quality of undergraduate education for sciences; Opportunities in and for Physicsbased industries. As a result of this seminar and subsequent recommendations to the Government, several initiatives like starting of the 5 year integrated MSc programmes in the country have taken place. The INSPIRE fellowship scheme, wherein bright students receive financial support for pursuing MSc, Ph.D and Post Doc. programmes is another outcome of the above seminar. All these schemes are in place and in the next ten years we would have created a rich pool of scientists who will take up fulltime research as their career. This I am sure will enhance the velocity of research. A

number of IISERs, CBS, NISER and new IITs have also come up in recent years. The positive results of these efforts will be seen in the next 10 years.

12. Scientific knowledge and innovation are contributing to approximately 50% of the economic growth in some of the advanced countries. What is the situation in India?

According to Dr. R. Chidambaram: "Scientific research generates new knowledge. Innovation adds economic value to this knowledge. Success in research brings prestige to scientists and to their country. Success in innovation brings prosperity to the country". Our Prime Minister has declared that the period 2011-2020 will be a decade of innovation. The recent science policy of the Government includes not only science and technology but also innovation. Innovation and creativity are the key components of any successful Science/Engineering research and development. Innovation will continue to play a significant role in all our R & D endeavours.

13. What are your personal memories that you would like to share with your younger colleagues and what is your future vision for BARC? Where do you see BARC 20 years from now?

BARC with its abundant talent of manpower, excellent infrastructure and ambience, should continue to hold a preeminent place in the nuclear science and technology map of the country. Multidisciplinary research is our strength and we must exploit this. We must continue to have a right mix of mission oriented programmes and R & D in frontier areas of science and engineering. We should also encourage our new colleagues to engage in higher studies and research in the first five years in addition to their involvement in R & D programmes. For faster implementation of some of the mega science projects, we coulddepute young colleagues to international laboratories, to

acquire requisite expertise (similar to what we did when we were constructing our research reactors in the initial stages). We must continue to have a sustained programme to spread awareness about BARC/DAE. In this connection, our young colleagues may be encouraged to visit universities/ colleges in general and their alma mater in particular, to deliver lectures and interact with academic institutions.

14. The BARC Newsletter has been the preferred channel of communication for BARC Scientists and Engineers for almost three decades now and in the last three years, it has undergone a major metamorphosis. Any suggestions to improve the quality and content?

The BARC newsletter is a powerful medium for spreading awareness about the R & D programmes and highlights of BARC. For taking this forward, one has to be clear about the targeted audience and the newsletter should cater to this group. In addition to the excellent articles which are being published, one could also add a regular page devoted to DAE activities, so that this information is also disseminated. We must encourage Senior BARC Scientists and Engineers to write for the newsletter. We could also regularly publish the R & D milestones reached and at the end of the year, provide a summary of the achievements for the whole year, in a nutshell. Feedback from the readers could be published. Depending on availability of space, we could publish about new colleagues who have joined BARC and those who have retired. This information can be spread over all the six issues. This practice is being followed by other DAE units in their house journals. I wish BARC newsletter continued success as it serves as the effective channel of communication for BARC scientists and engineers.

Thirty Years of Research Activities through the Pages of the BARC Newsletter

K. Bhanumurthy and Sangeeta Deokattey

Scientific Information Resource Division

Abstract

The objective of this paper is to focus on the development of BARC Newsletter from simple 4-page content in August 1983 to the present 50 page July/August 2013 issue. BARC Newsletter has captured innovations in R&D activities of BARC and has kept pace with achievements of BARC. There have been several changes in the last 30 years, but the essence and principles of publication have not changed, and it has managed to keep its readers enthralled all these years.

The Beginning: The first issue of the BARC Newsletter appeared on 1st August, 1983. At that time it was a simple 4-page layout and printed in Black & White. During the first 17 years of its journey, it has published R&D activities from different Groups, opinions of Senior Scientists and also included names of scientists and their work which brought laurels to BARC. The content went on increasing with increase in the outstanding achievements of BARC and some of these activities as reflected in the BARC Newsletter are summarized below:

- 1st August, 1983: Publication of the first issue of the BARC Newsletter

- 9th August, 1985: Dhruva goes critical

- 30th Oct., 1985: Fast Breeder Test Reactor goes critical

- July 1987: BARC develops graphite materials for use in Rockets

- Dec. 1988: Inauguration of the Medium Energy Heavy Ion Accelerator (MEHIA) Facility

- Nov. 1990: Purnima III attains criticality.

The Second Decade (1991-2000): The BARC Newsletter during this period had kept pace with developments in printing technology and a 4 colour format was adopted for a more aesthetic look. The total number of pages increased from 4 to 8 and it also included a Contents table for better readability. The quality of figures improved along with the number of research articles. The research areas covered in the BARC Newsletter represented the multidisciplinary nature of R&D in BARC and it also continued to publish information on award winners. The DAE Awards Scheme was introduced in 1992. Most of the important developments in this period were included in the BARC Newsletter and a few are summarized below:

- Feb. 1991: One Millionth Consignment of Radioisotope was produced at Trombay and delivered to Tata Memorial Centre

- Aug. 1992: BARC develops a coolant channel inspection system (BARCIS Mark 1) for 235MWe PHWRs

- July 1993: BARC develops Boron carbide and Boron carbide associated composites

- Aug. 1995: Special issue of the BARC Newsletter dedicated to Food Irradiation

- May 1996: Installation of GRACE (Gamma Ray Astrophysics Cerenkov Experiment) Telescope at Mount Abu

- May 1998: Report of Pokhran tests

- Aug. 1999: Solid Storage Surveillance Facility at Tarapur commissioned.

The Third Decade (2001-2009): The coverage of feature articles increased along with a better design of front and back covers. The total number of articles published also increased (1-2 articles in every issue) in addition to coverage of important scientific events. The decade culminated in the birth centenary celebrations of our Founder, Dr. Homi Jehangir Bhabha in October 2009. The major developments that need special mention are given below:

- Jan. 2003: Inauguration of the Waste Immobilization Plant at Trombay

- Feb. 2005: BARC Develops Cobalt-60 Teletherapy Machine for Cancer Treatment

- Dec. 2005: Supercomputing Facility inaugurated at BARC

- Jan. 2006: Golden Jubilee year of BARC inaugurated

- Sep. 2008: Export of Radiation-processed Indian mangoes to USA

BARC Newsletter between 2010 and now: Major changes were introduced in the BARC Newsletter with the formation of the BARC Newsletter Editorial Committee. The frequency changed from monthly to bimonthly and the format and structure gave an appearance of a journal. The articles (reviewed) were classified as Research Articles, Technology Development Articles and Feature articles. In July-August 2010, the BARC Newsletter was allotted the international ISSN Number: 0976-2108 thus giving it a unique identity. The online version began to be made available through three separate portals: Saraswati, BTS and through BARC websites. In October 2010, the Founder's day Special Issue was printed and released for the first time on a CD. A new feature, "Brief Communications" was introduced in the Newsletter from 2012. An online portal "BARC Publications" was developed for submission of articles to the BARC Newsletter.

Future Direction: Change is an inherent strength of any publication and much has changed over a period of three decades for the BARC Newsletter. But one thing that has remained constant is the standard and quality of its publication. Even today, sincere efforts are being made to reflect and mirror the achievements of BARC and it will continue to be done in future too.

We are indeed grateful to all the researchers who have contributed articles and to the editors who have spent their quality time to make it look like what it is today.

Aqueous Dye Lasers: A Supramolecular Approach Toward Sustained High Power Operation

Alok K. Ray, S. Kundu, S. Sasikumar and K. Dasgupta
Laser & Plasma Technology Division
and
S. K. Nayak
Bio-organic Division

Abstract

Development of technologically viable dispersive additives which would not only prevent detrimental aggregation of laser dyes in water, but also improve its efficiency and photostability, has remained an attractive and challenging goal in the development and use of high pulse repetition frequency (prf) dye lasers. Recently, encapsulation dynamics of a few rhodamine, pyrromethene and coumarin dyes into the nano-cavity of a molecular container cucurbit[7]uril(CB[7]) were investigated extensively by us using absorption, steady state and time resolved fluorescence, ^{1}H and ^{13}C NMR, MALDI-TOF spectroscopy techniques and its applications in aqueous dye lasers were evaluated by constructed GIG-configured pulsed dye lasers. Based upon the observations of a large improvement in photostability and efficiency of aqueous rhodamine B dye lasers, pumped by a frequency-doubled, low prf (10 Hz) Nd-YAG (532 nm) laser, design specifications were determined for testing this system in high prf (>10 kHz) dye lasers, pumped by the yellow (578 nm) component of copper vapor lasers. The requirement for a large quantity of spectroscopy grade CB[7] (~40 gm, cost ~ Rs. 1.3 lakh/gm) for use in the high prf dye laser experiments were achieved through an indigenous synthesis effort.

Introduction

The development of efficient and photostable high pulse-repetition-frequency (prf), as well as, high average-power, narrow line width tunable dye laser systems with sustainable operation is important in several applications in nuclear science and technology. Operation of such high prf liquid dye lasers, with water in place of commonly used toxic and inflammable organic solvents, would offer substantial advantages including reduced safety issues, higher Power capability and better beam quality [1a-b]. The functional advantages arise from the better thermal and thermo-optic characteristics of water that can be represented by a thermo-optic figure of merit, $F = [k\rho s/(dn/dT)]$, where k, ρ and s are thermal conductivity, density and specific heat of the solvent, respectively, and dn/dT is the thermo-optic refractive index coefficient. A few common dye solvents such as propanol, ethanol, water and heavy water have 'F' values 910, 912, 27714 and 39360, respectively. In particular, highly-monochromatic and high power dye lasers operating in continuous working mode or at high prf, stand to gain significantly with use of normal or heavy water solvent. The performance of such lasers depend sensitively on the thermally induced optical inhomogeneity in the gain medium which cannot be eliminated completely by dye flow circulation. Also, aqueous solvents generally produce a red shift in the dye laser tuning range, which may provide an added advantage for some specific wavelength generation.

However, dye molecule dissolved in water forms non-fluorescent aggregates owing to the highly polar nature of water, thereby drastically degrading laser performance. Many dispersive additives such as host micelle and β-cyclodextrin or low-polarity co-solvent such as propanol were examined earlier by us as well as by other researchers. These approaches have so far shown limited success, either requiring large concentration (10's of mM) of the additive leading to partial quenching of dye fluorescence or, substantially reduced F value of dye solutions [2a-c].

Based upon a preliminary study initiated by us in collaboration with RPCD testing the feasibility of using the latest molecular container cucurbit[7]uril (CB[7]) in a Rhodamine 6G dye laser, we have carried out an extensive series of investigations on the use of CB[7] in dye lasers. Accordingly, encapsulation dynamics of some important laser dyes with the CB[7] were characterized using various spectroscopy techniques, as well as, through modeling approaches, followed by laser studies of these aqueous active media pumped by the second harmonic (532 nm) of a pulsed Nd:YAG laser [3a-e]. Simultaneously, development of an indigenous procedure for bulk synthesis and purification of dispersive material CB[7] was undertaken. In this article, we present a brief review of this work employing widely used rhodamine B (RhB), Kiton Red Sulfur (KRS) and coumarin 1 (C1) laser dyes. It was found that aqueous RhB system with synthesized additive CB[7] provides higher photostability ($\sim$2.5 times) and efficiency ($\sim$17% more) in a red shifted tuning range, in comparison to that using ethanol as solvent. These studies established RhB-CB[7]-water combination as a potential active medium for high average power dye laser operation, enabled the selection of design parameters, and led to the production of sufficient quantity of pure CB[7] in collaboration with ICT, Mumbai, for conducting technology deployment tests in dye lasers in BARC.

Materials

High purity RhB, KRS and C1 laser dyes were procured while CB[7] was synthesized to carry out the intended studies (Fig.1 illustrates the molecular structures). The detailed procedures for synthesis and purification of CB[7] are protected by many patents. The reported procedure of synthesis by acid catalyzed condensation always leads to the formation of a mixture of CB[5], CB[6], and CB[7] with CB[6] as the major product. Experimentally, the major difficulty lies in the separation of CB[7] from its water soluble homologue CB[5], these usually co-crystallize together as a mixture. After several trials, limited information available on procedures for synthesis and purification has been optimized to get spectroscopic grade CB[7] in 12-15% yield [4a], which led to the bulk synthesis of CB[7]at the Dyestuff Technology Dept., ICT, Mumbai through a collaborative ATC-BRNS project. Finally, the absolute purity of CB[7] was unequivocally confirmed by NMR, MALDI-TOFMS along with spectrophotometric titration using an organometallic host [4b], which has a strong binding affinity for CB[7] (K $>10^8$), but no such binding with CB[5].

Encapsulation dynamics of dyes with CB[7]

Absorption, steady-state and time-resolved fluorescence spectra of aqueous dyes showed a large increase in their fluorescence quantum yield (Φ_f) and lifetime (τ_f) along with red shifted absorption/emission profile and reduced non-radiative decay
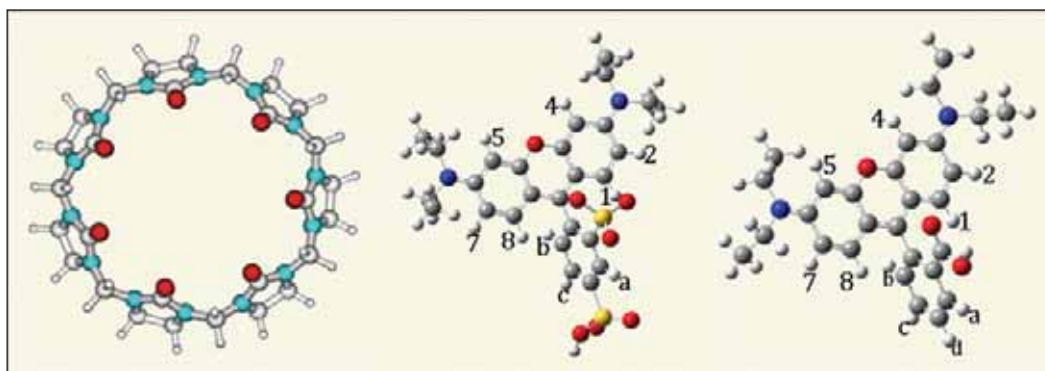

Fig. 1: Optimized ground state structures of (a) host (CB[7]) (top view), and dyes (b) RhB and (c) KRS. Color code: red, Oxygen; blue, Nitrogen; Sulfur, yellow and gray, Carbon (large) and Hydrogen (small)
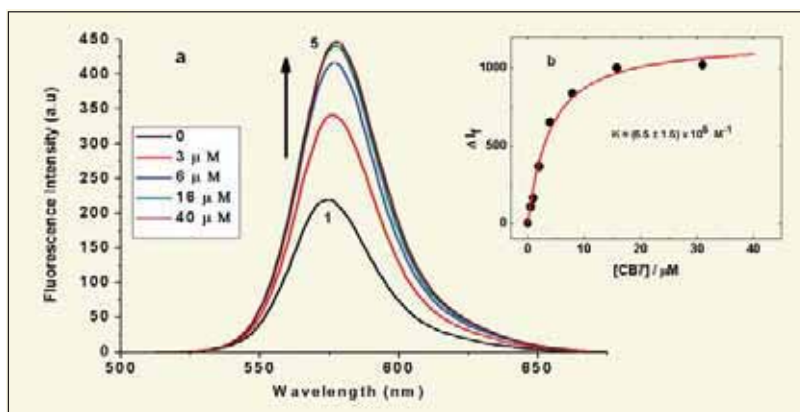
Fig. 2: (a) Fluorescence spectra of RhB (∼3.5 ìm) in water with CB[7]. Inset figure (b) Fluorescence titration curve of RhB in the presence of CB[7] (•). The solid line represents the fitted curve corresponding to 1:1 complex formation, with a binding constant, $K=(6.5 \pm 1.5) \times 10^5$ M^{-1}.

rate (k_{nr}), in the presence of CB[7]. Analysis of photophysical properties of the dyes with CB[7] suggested the formation of 1:1 dye-CB[7] complex with a high binding constant ($K>10^5$ M^{-1}) for RhB (Fig. 2), KRS and C1 [3]. The complex formation with tighter binding and rotation of the whole complex as a single entity was corroborated further by the observation of increase in rotational relaxation times (τ_{rot}) of these dyes in presence of CB[7], and a
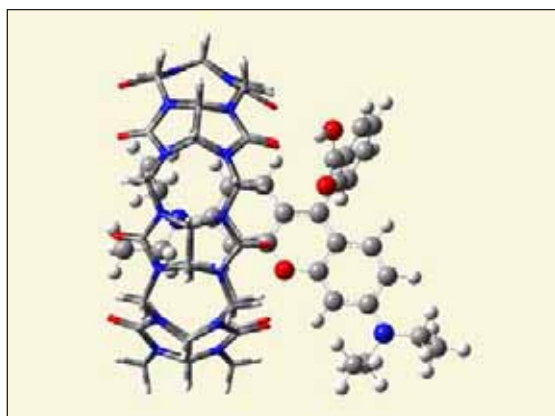

Fig. 3: Optimized ground-state structure of the RhB-CB[7] complex, calculated by DFT at the B3LYP/6-31G(d,p) level of theory. Color code: red, Oxygen; blue, Nitrogen; and gray, Carbon (large) and Hydrogen (small)

close agreement with calculated values of τ_{rot} for the dye-CB[7] complex, while considering the inclusion of the dye molecule inside the CB[7] cavity [5]. Additionally, the complex formation was found

to beneficially prevent reduction of fluorescence yield with increase in temperature of dye solutions in the region 16-25°C [5c].

Aqueous dye lasers

Comparative laser performances of both the rhodamine dyes, RhB and KRS, were evaluated in normal, heavy water and ethanol media, using a constructed [6] pulsed dye laser oscillator with a grating of 2400 lines/mm and a 25X, 4-prisms beam expander (PBE), which was transversely excited by the second harmonic of a Q-switched (fwhm ∼ 6ns) Nd:YAG laser. The vertically polarized pump beam was line focused onto a flow-through dye cell by a combination of plano-concave and cylindrical lenses. An intra-cavity half-wave (λ/2) plate, in the dispersive wing of the resonator between the dye cell and the PBE, maximized both the grating diffraction efficiency and the PBE transmission while ensuring maximum extraction efficiency from the gain medium [6a]. The concentrations of dyes were optimized to have similar OD (∼8) at pump wavelength, that also produced high efficiency and a near-circular output beam profile. The dye laser tuning wavelengths were obtained by rotating the tuning mirror.

Initially, the performances of synthesized and imported samples of CB[7] were evaluated using an aqueous RhB dye laser and was found to be comparable (Fig. 4). Both the RhB and KRS dyes showed maximum peak laser efficiency at 1:1 molar ratio of dye:CB[7] supporting the hypothesis of 1:1 complex formation. The peak laser efficiencies of both the dyes were found to be significantly higher in the aqueous CB[7] media than that in ethanol (Fig. 5 for RhB dye). The observed increase in laser efficiency of dyes in water/CB[7] system may be attributed to the reduced de-polarization rate
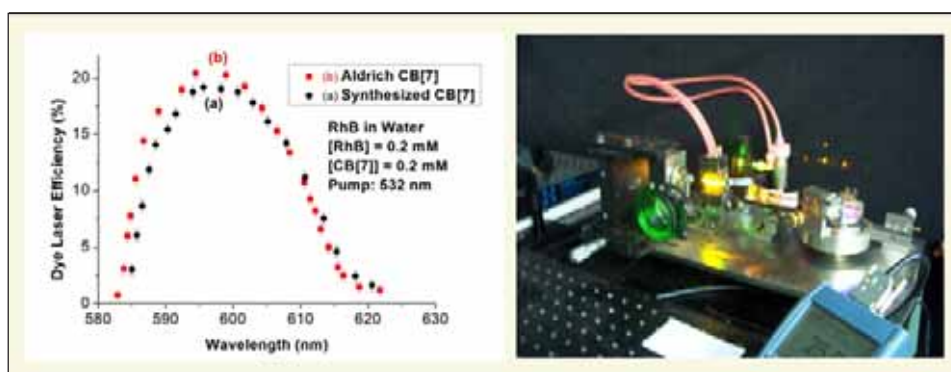
Fig. 4: Comparative performances of CB[7] in RhB dye laser, (a) synthesized and (b) imported sample. Photograph shows the constructed GIG-configured dye laser set up, pumped by Nd-YAG (532 nm) laser, used for this work.
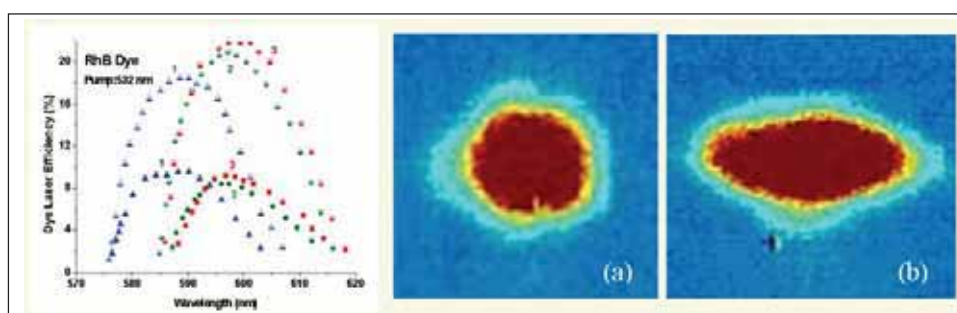

Fig. 5: Dye laser tuning curves of RhB (0.2 mM) using (1) ethanol, (2) water-CB[7] , and (3) heavy water-CB[7], [CB7] =(0.2 mM). Enhancement in RhB dye laser efficiencies, with intra-cavity λ/2 plate, using (1) ethanol, (2) water and (3) heavy water are represented by half filled blue triangles, green circles and red squares, respectively. The pump pulse energy was 6.3 mJ. Superior spatial profile of the dye laser output using (a) water-CB[7] compared to (b) ethanol is illustrated.

$(1/\tau_{rot})$ of the complexed dye molecules (Table 1), which are excited with a predominant vertical distribution of dipoles by the vertically polarized pump beam. This is also the preferred orientation for efficient interaction with the vertically polarized intra-cavity signal produced by the particular design [6b] of the cavity. Another significant observation was the increase in photostability (Φ_{PS}) of the dyes in water/CB[7] system (2.5 to 5 times) than that in ethanol. The enhanced photostability of the dyes in water-CB[7] system can be explained by their encapsulation into the chemically inert, non-polar environment of CB[7] cavity and its rigidizing effect, which may reduce reaction rates of dyes with reactive species produced from solvent or dissolved

Table 1: Photophysical and dye laser (DL) parameters of RhB and KRS. [a] fluorescence standard

Dye/solvent/ additive	λ_{abs}^{max} (nm)	λ_{em}^{max} (nm)	Φ_f	τ_f (ns)	k_r (10^8) s^{-1}	k_{nr} (10^8) s^{-1}	τ_{rot} (ps)	Laser Tuning range (nm)	λ_L (nm)	η (%)	Φ_{PS} (10^5)
RhB/EtOH	543	576	0.70	2.8	2.5	1.07	267	576-607	588	18.4	2.4
RhB/H$_2$O	554	578	0.32	1.5	2.1	4.53	214		597	6	
RhB/H$_2$O/CB[7]	556	581	0.88	3.5	2.5	0.34	518	585-616	597	21	6.3
KRS/EtOH	555	574	0.69[a]	3.8	1.8	0.82	265	577-604	588	16.5	1.3
KRS/H$_2$O	565	586	0.27	1.5	1.8	4.87	212		588	5	
KRS/H$_2$O/CB[7]	567	588	0.60	3.3	1.8	1.21	473	592-643	603	20.6	6.7

λ_L: peak DL wavelength, η = Peak DL efficiency

oxygen during laser excitation. Rigidization may also reduce inter-system crossing rate that produces reactive dye molecules in the triplet state, thereby improving photostability. The photophysical and laser properties of aqueous RhB and KRS dyes, in absence and presence of CB[7], are listed in Table 1, along with that in ethanol.

The results show that the CB[7]-water system is superior to ethanol, particularly for achieving sustained and efficient operation when used in, high-power dye lasers, where the dye solution would be subjected to high rate of photo-exposure tending to produce a faster rate of photo-degradation.

Conclusion

In conclusion, aqueous rhodamine dye lasers with higher efficiency and photostability, compared to ethanol solutions were demonstrated, using locally synthesized molecular container additive CB[7]. The successful development of techniques for bulk synthesis and purification of CB[7] has made this approach suitable for technology development of high average power aqueous dye lasers. This work has established RhB-CB[7]-water system an attractive active media with superior thermo-optic characteristics aimed at sustained and efficient operation in high-average-power dye lasers.

Acknowledgements

References

1. a) D. Klick (1990) Industrial application of dye lasers, in *Dye Laser Principles with Applications*, 345-398, (Academic, New York), b) C. E. Webb(1991) High power dye lasers pumped by copper vapo*r lasers, in High-Power Dye Lasers, F.* J. Duarte, ed., Vol. 65 of Springer Series in Optical Sciences, Springer-Verlag, Berlin, pp. 177-179.

2. a) K. Igarshi, M. Maeda, T. Takao, M. Uchiumi, I. Oki, and K.Shimamoto (1995), Jpn. J. Appl. Phys. 34, 3093-3096, b) A. K. Ray, S. Sinha, S. Kundu, S. Kumar, S. K. S. Nair, T. Pal and K. Dasgupta (2002), Appl. Opt.-LP 41, 1704, c) A. K. Ray, S. Sinha, S. Kundu, S. Sasikumar, K. Dasgupta (2007), Appl. Phys. B 87 , 489-495.

3. a) A. L. Koner, W. M. Nau (2007), Supramol. Chem. 19, 55-66, b) J. Mohanty, H. Pal, A. K. Ray, S. Kumar and W. M. Nau (2007), ChemPhysChem 8, 54-56, c) J. Mohanty, K. Jagtap, A. K. Ray, W.M. Nau and H. Pal (2010), ChemPhysChem, 11, 3333-3338, d) Monika Gupta, D.K. Maity, M.K. Singh, S.K. Nayak and A.K. Ray (2012), J. Phys. Chem. B, 116 , 5551-5558, e) J.K. Khedkar, K.K. Jagtap, R.V. Pinjari, A.K. Ray and S.P. Gejji (2012), J. Mol. Modelling, 18, 3743-3750.

4. a) Deepak R. Boraste, Monika Gupta, Ganapati Shankarling, Alok K. Ray and Sandip. K. Nayak (2013), National Laser Symposium-21, CP-01-45, b) Song Yi and Angel E. Kaifer (2011), J. Org. Chem., 76, 10275-10278.

5. a) K. K. Jagtap, Monika Gupta, Mamata Kombrabail and A. K. Ray (2013), National Laser Symposium-21, CP-01-35, b) Monika Gupta, K. K. Jagtap, V. Sudarshan and A. K. Ray (2013), National Laser Symposium-21, CP-03-29, c) K. K. Jagtap, D. K. Maity, A. K. Ray, K. Dasgupta, S. K. Ghosh (2011), *Appl. Phys. B*, 103, 917.

6. a) S. Kundu, A. K. Ray, S. Sinha, S. Sasikumar, S.K.S. Nair and K. Dasgupta (1999), National Laser Symposium-8, b) K. Dasgupta (1991), Ph.D. Thesis, Univ. of Bombay.

Significance of DNA repair proteins presence in multiprotein complex and its importance in radiation resistance of *Deinococcus radiodurans.*

Swathi Kota and H. S. Misra
Molecular Biology Division

Abstract

Deinococcus radiodurans has an efficient DNA double strand break (DSB) repair mechanism, which helps it to mend hundreds of DSBs produced after exposure to the exceptionally high doses of ionizing radiation and shows no measurable loss of cell viability. This tolerance is well above the DSB tolerance by any other organism. The better catalytic efficiency of different proteins associated with DSB repair could come by their existence in close vicinity and through protein-protein interactions, which may be important for the extreme radioresistance of this bacterium. Keeping this hypothesis in mind, we isolated a multiprotein DNA processing complex from *D. radiodurans*, identified its components and demonstrated the roles of some of these components in the radioresistance of this bacterium.

Introduction

Proteins are the biological workhorses performing variety of functions in the cells. A large number of biochemical, molecular and cellular processes are known to be performed by the assemblies of 10 or more proteins (Alberts, 1998). These multiprotein assemblies help in enhancing the speed and specificity of the reactions. Proteins present in multiprotein complexes acquire new functions and even unknown proteins have been characterized based on the functions of their interacting partners. Multiprotein complexes may also act as depots to release protein components depending upon the requirement of the cells. Recent advances in protein tagging methods followed by protein identification by mass spectrometry have helped in deciphering the protein-protein interactions in several organisms including yeast, *E. coli* and human cell lines.

Ionizing radiation produces DNA double strand breaks (DSBs), a most severe form of DNA damage in living cells. Density of DSBs determines whether cells would have some undamaged copy of the genome or not, and that eventually determines the DSB repair efficiency of the cells. The extremely high

dose of ionizing radiation would cause extensive damage to DNA leaving almost no intact DNA strand and any defect in DSB repair would eventually leads to cell death. Therefore, an organism that could sustain under extreme doses of gamma radiation exposure would be expected to have the highly efficient mechanisms to combat the deleterious effects of ionizing radiation. In eukaryotes, one of the early steps of DNA damage response (DDR) is marked by the synthesis of proteins required in DNA damage induced signal transduction, DNA recombination and repair functions and those associate with oxidative stress tolerance. It is believed that the synthesis of different proteins required for combating the radiation effects are produced in an ordered and hierarchical fashions (Harper and Elledge, 2007). This involves extensive and programmed protein–protein interactions triggered by a variety of post-translational modifications like phosphorylation, ubiquitylation, SUMOylation, acetylation etc. The DDR helps the cells to shelter the broken DNA ends from decay, prevents illegitimate repair processes and amplifies the DNA

damage induced signal transduction (Nussenzweig and Nussenzweig, 2010). Accumulation of a large number of DDR factors at the sites of DNA damage also provides the cells with a "toolbox" containing all available enzymatic activities relevant for DNA repair and other cellular metabolism.

Deinococcus radiodurans is characterized for its exceptional ability to withstand the lethal and mutagenic effects of DNA-damaging agents including ionizing radiation. This phenotype has been attributed to the mechanisms contributing to the efficient DSB repair and strong oxidative stress tolerance. It survives from nearly 200 DSBs and 3000 single strand break without a measurable loss of cell viability (Battista, 2000). *D. radiodurans* genome exists in donut-like toroidal structure and this compacted form of nucleoid remains unaltered even after exposure to high-dose of γ radiation (Levin-Zaidman *et al.*, 2003). The genome sequence of *D. radiodurans* is known. It contains the DNA repair proteins almost similar to the radiosensitive bacterium, *E. coli* (White *et al.*, 1999), except the absence of components required for the RecBC recombination pathway of DSB repair. The transcriptome analysis of *Deinococcus* cells exposed to acute doses of gamma radiation and desiccation had also revealed the enhanced expression of several uncharacterized genes (Liu *et al.*, 2003). The other mechanism that supports the extreme doses of ionizing radiation in *D. radiodurans* is its ability to tolerate higher levels of oxidative stress. Different factors that contribute to its oxidative stress tolerance are the exceptionally high quality antioxidant enzymes i.e. catalase and superoxide dismutase (Markillie *et al.*, 1999), antioxidant metabolites like Deinoxanthin, a major carotenoid having better scavenging ability than their counterparts (Tian *et al.*, 2008) and the pyroloquinoline-quinone (PQQ), that scavenges reactive oxygen species at a rate constant comparable with the commercially available antioxidants Trolox™ and vitamin C (Misra *et al.,* 2004). The roles of pyrroloquinoline quinone in oxidative stress tolerance of *D. radiodurans* has been

demonstrated (Rajpurohit *et al.*, 2008). Recently, it has been shown that *D. radiodurans* also accumulates Mn(II) with a much higher intracellular ratio of Mn/Fe as compared to other bacteria. Mn(II) also forms complex with small molecules like inorganic phosphate, small peptides and nucleotides in this bacterium and such types of Mn complexes have been shown protecting the biomolecules mainly proteins, from oxidative damage effect of gamma radiation *in vitro* (Daly *et al.*, 2010).

DNA double strand break repair in *D. radiodurans.*

In bacteria, the RecBCD and /or RecFOR pathways of homologous recombination are involved in DSBs repair (Wyman and Kanaar, 2006). In both these pathways, different proteins help in loading RecA, a key recombination protein, to DNA damage site, which then catalyzes homology search and strand exchange reactions (Kowalczykowski *et al.*, 1994) required in DSB repair. Very interestingly, the RecBC enzymes, which have been termed as DSB repair enzyme in all other bacteria studied till date, are absent in *D.radiodurans*. Except, RecB and RecC homologues, and their suppressors like *sbcA* and *sbcB*, all other components of both classical homologous recombination repair pathways i.e. RecBC and RecF are present in the genome of this bacterium (White *et al.*, 1999). Recently, a unique mechanism called extended synthesis dependent strand annealing (ESDSA) was suggested contributing to efficient DSB repair and radiation resistance in *D. radiodurans* (Zahradka *et al.*, 2006). The ESDSA is a multi step process, which would involve a large number of enzymes. The involvements of some of the known DNA repair and recombination proteins in ESDSA have been shown. Genome of this bacterium exists in toroidal form, and is speculated that the enzymes /proteins located in vicinity to the DSBs in toroidal genome could repair these breaks at a much faster rate than if these are scattered with the cellular milieu. Thus, the classical homologous recombination repair, ESDSA mechanisms of DSB repair and even direct repair of breaks produced on

toroidal genome would be expected to require a large number of protein candidates. These may work efficiently if they are present together. Since, DSB repair is highly efficient in this bacterium, the possibility of various DNA metabolic proteins existing together could be hypothesized. So, we studied the possibility of the existence of multiprotein complexes and their relevance to radiation resistance in *D. radiodurans*.

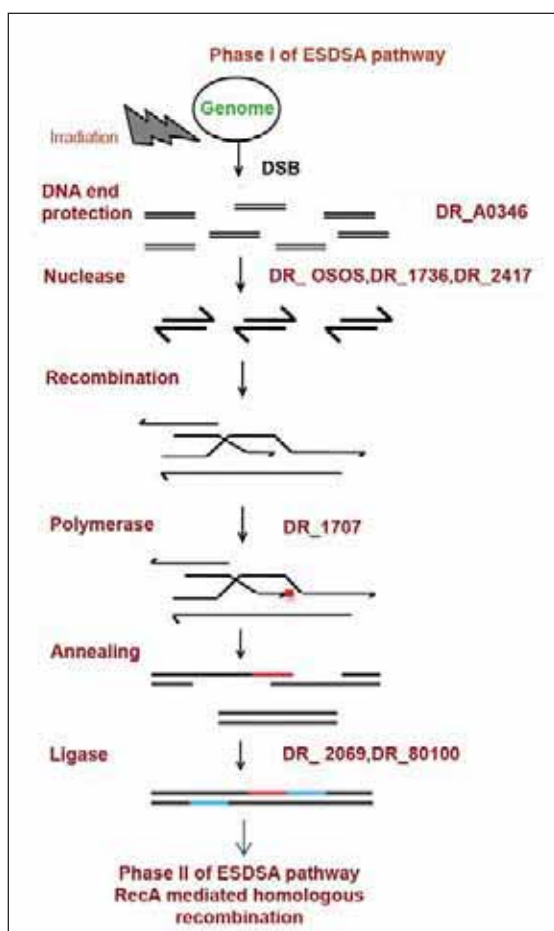## DNA processing complex was isolated from *D. radiodurans*

Level of radioresistance in stationary phase cells of *D. radiodurans* is reported to be nearly 2 folds higher than the exponentially growing cells (Minton, 1994). The cell free extract of stationary phase cells of *D. radiodurans* was fractionated using molecular sieve column chromatography. A parallel experiment was also carried out with cell free extract of radiosensitive bacterium *E. coli*. The protein fractions collected from the cell free extracts of *E. coli* and *Deinococcus* formed distinct peaks. One such fraction from both *E. coli* and *D. radiodurans* proteins showed relaxation of superhelical form of plasmid i.e. toposiomerase type enzymatic activity. The integrity of this complex was ascertained using both analytical and biophysical techniques. Further the complex from *Deinococcus* showed ATP inhibition of nuclease activity while *E.coli* sample showed ATP stimulation of nuclease activity. *E. coli* sample also showed presence of RecA, which was absent in *Deinococcus* complex. Thus, the complexes isolated from two bacterium with entirely different DNA damage response have topoisomerase type function but they differ in terms of ATP regulation of nucleolytic (DNA processing) activity and also with regards to the presence of RecA, the key enzyme in recombination repair of DSBs. In case of *Deinococcus*, the high-energy phosphate like ATP might help the organism in controlling indiscriminate DNA degradation and loss of genetic information could be suggested.

Biochemical activity characterization of the multiprotein complex from *D. radiodurans* showed the presence of some of the DNA metabolic functions that are integral to any mechanism of DNA repair. Notable ones are (i) the DNA synthetic functions including both DNA polymerization and DNA end joining, and (ii) DNA degradation / processing and topology relaxation functions as measured by *in vitro* activity assays. Complex also contains phosphoproteins and shows protein kinase activity (Fig.1). FT-MS analysis of complex components shows the presence of 24 proteins encoded in the genome of *D. radiodurans* (Table 1). These include some of the known proteins like DNA polymerase I, PprA, Topoisomerase IB, DnaK, and several uncharacterized proteins including DRB0100 a putative ATP type DNA ligase, and DR0505, a hypothetical protein containing functional motifs (PDE) for diesterase activity. Complex shows DNA end-joining activity only in presence of ATP and not with NAD. Some of the proteins of multiprotein complex like PprA (Narumi *et al.*, 2004), DNA polymerase I (Slade *et al.*, 2009) and topoisomerase IB (Krogh and Shuman, 2002) of this bacterium have been characterized independently, and their roles in radiation resistance have been demonstrated. We further studied PprA (Kota and Misra, 2006), DRB0100 (Kota *et al.*, 2010a) and DR0505 (Kota *et al.*, 2010b) detected in this complex and demonstrated the possible roles of these proteins in bacterial response to oxidative stress and DNA damage produced by gamma radiation.

Significance of proteins being together for efficient function

The DRB0100 polypeptide, a putative ATP type DNA ligase was detected in multiprotein complex. The coding sequence of DRB0100 was cloned and expressed in *E. coli*. The recombinant DRB0100 protein was purified to homogeneity and checked for ligase activity. Purified protein did not show DNA end joining activity with double stranded linear DNA substrate. Independent study has also confirmed that the purified form of DRB0100 is inactive (Blasius *et al.,* 2007). It may be noted that the complex in
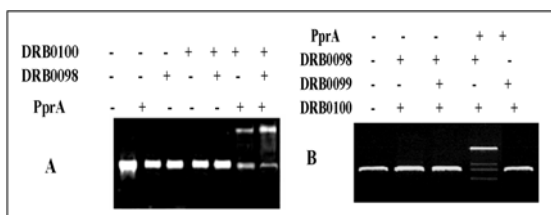
Fig. 1: Different protein components of DNA processing complex characterized for their *in vitro* activities which are integral to Extended Synthesis Dependent Strand Annealing (ESDSA) pathway of DSB repair in *D. radiodurans*. Ionizing radiation produces DNA double strand breaks (DSB) in the genome. The DNA is protected from indiscriminate chewing by proteins like PprA (DR_A0346). Nucleases process DNA (DR_0505, DR_1736, DR_2417) to generate 3' overhang fragments, which recombine with near homologous fragments. DNA Polymerases (DR_1707) extends the DNA, which anneals with complementary stands and joined with ligases (DR_2069, DR_B0100) to generate long intermediate fragments. This follows the RecA mediated homologous recombination to generate full-length genome without any errors

Table 1: Mass spectrometric analysis of protein complex components

Annotated ORFs in the host genome	Protein size (~KDa)	*Deinococal* protein identity
DR0116	13.7	Hypothetical protein
DR0129	67.9	DnaK protein
DR0505	59.3	5'-Nucleotidase family protein
DR0644	20.7	Hypothetical protein
DR0672	17.1	Hypothetical protein
DR0673	19.9	Hypothetical protein
DR0690	38.9	Hypothetical topoisomerase
DR0691	27.0	Hypothetical protein
DR0969	46.1	Hypothetical protein
DR0972	23.4	Conserved hypothetical protein
DR1124	42.6	SLH family protein
DR1483	32.2	Hypothetical protein
DR1706	12.7	Hypothetical protein
DR1707	102.6	DNA-dependent DNA polymerase
DR1736	73.1	Cylic nucleotide 2'-phosphodiesterase
DR1768	15.0	Hypothetical protein
DR2069	75.4	DNA ligase
DR2310	84.2	Hypothetical protein
DR2417m	63.5	Conserved hypothetical protein
DR2527	20.2	tIypothetical protein
DR2563	7.8	Hypothetical protein
DR A0346	32.0	PprA
DRB0067	109.7	Putative extracellular nuclease
DRBOI00	24.3	Putative DNA ligase

which this protein was detected also had shown the ATP stimulated DNA end joining function *in vitro*. On the other hand, the PprA protein, another component of multiprotein complex was shown to stimulate both NAD and ATP dependent DNA ligases *in vitro* (Narumi *et al.*, 2004). Therefore, the possibility that the DRB0100 expresses its DNA end-

joining activity in presence of PprA was hypothesized and checked. We observed that the purified DRB0100 alone had no activity. But when purified DRB0100 was incubated with purified PprA protein, it showed DNA end-joining activity (Fig. 2). The functional complementation to the loss of radioresistance phenotype of *drb0100* mutant by DRB0100 *in trans* also required all the three proteins of *drb0100* operon (DRB0098, DRB0099 & DRB0100), where as these proteins failed individually to complement *drb0100* mutant phenotype. This suggested that the loss of gamma radiation resistance in *drb0100* mutant was not solely due to loss of DRB0100 alone but also due to the combined loss of all three components of operon. These results strongly suggested that DRB0100 functions in form

Fig. 2: DNA end-joining activity assay of recombinant DRB0100 (LigB) in presence of its operon components like DRB0099 and DRB0098, and the PprA protein. The purified recombinant protein as assayed with linear plasmid substrate (B) and with 1kb PCR amplified DNA substrate (A). The effect of PprA (A) and DRB0099 (B) on DRB0098- supported ligation efficiency of LigB was assayed on agarose gel

of a complex and it requires PprA, another component of the complex for its activity at least *in vitro*. Thus we demonstrated the functional significance of several proteins being together in multiprotein complex (Kota *et al.*, 2010a; Kota *et al.*, 2010b; Kota and Misra, 2006) for their efficient functions at least by taking DNA ligase activity of DRB0100 as an example.

Conclusion

The existence of multiprotein DNA processing complex in *Deinococcus* whose genome forms the highly compacted nucleoid structure and requires several proteins to come together for efficient and accurate DSB repair becomes much more relevant. We demonstrated that a few DNA repair proteins, some of the hypothetical proteins, and DnaK a molecular chaperon, are present together in the form of a multiprotein complex in *D. radiodurans*. Two of the uncharacterized components of the complex such as DRB0100 and DR0505 were assigned functions and their roles in extraordinary radiation resistance of this bacterium have been ascertained. The ATP mediated fine balance between DNA degradation by the presence of the nuclease like DR0505, and DNA synthetic function by the presence of DRB0100 in this complex has been suggested. Likewise, this complex is found to contain another mutually incompatible functions like protein phosphorylation by the presence of protein kinase and dephosphorylation by phosphodiesterase like

DR0505. Recently, the role of a membrane associated protein kinase (DR2518) in radiation resistance of *Deinococcus* has been shown (Rajpurohit and Misra, 2010). Therefore, the possibility of different activities of complex being regulated by protein phosphorylation/ dephosphorylation through coordinated balance of the protein kinases and phosphodiesterase activity stiochiometry may be speculated. This study has therefore, provided fewer answers but has generated a number of intriguing and potentially interesting questions. Some of these are (i) what triggers the formation of such macromolecular complexes in this bacterium and how various activities of the proteins are regulated in the complex, (ii) how protein kinase and esterase enzymes are functioning together in complex, (iii) roles of DnaK, and other proteins having protein-protein interacting domains in stabilization of the integrity of the complex, and (iv) the *in vivo* presence of such complex and its significance in radiation resistance and DSB repair of *D. radiodurans*, would be worth ascertaining.

References

1. Alberts, B. (1998) The cell as a collection of protein machines: preparing the next generation of molecular biologists. *Cell* 92: 291-294

2. Battista,J.R. (2000) Radiation resistance: the fragments that remain. *Curr Biol* 10: R204-R205.

3. Blasius, M., Buob, R., Shevelev, I. V., and Hubscher, U. (2007) Enzymes involved in DNA ligation and end- healing in the radioresistant bacterium, *Deinococcus radiodurans*. *BMC Mol. Biol.* 8, 69.

4. Daly,M.J., Gaidamakova,E.K., Matrosova,V.Y., Kiang,J.G., Fukumoto,R., Lee,D.Y. *et al.* (2010) Small-molecule antioxidant proteome-shields in *Deinococcus radiodurans*. *PLoS One* 5: e12570.

5. Harper,J.W., and Elledge,S.J. (2007) The DNA damage response: ten years after. *Mol Cell* 28: 739-745.

6. Kota,S., Kamble,V.A., Rajpurohit,Y.S., and Misra,H.S. (2010a) ATP-type DNA ligase requires

other proteins for its activity in vitro and its operon components for radiation resistance in *Deinococcus radiodurans in vivo*. *Biochem Cell Biol* 88: 783-790.

7. Kota,S., Kumar,C.V., and Misra,H.S. (2010b) Characterization of an ATP-regulated DNA-processing enzyme and thermotolerant phosphoesterase in the radioresistant bacterium *Deinococcus radiodurans*. *Biochem J* 431: 149-157.

8. Kota,S., and Misra,H.S. (2006) PprA: A protein implicated in radioresistance of *Deinococcus radiodurans* stimulates catalase activity in Escherichia coli. *Appl Microbiol Biotechnol* 72: 790-796.

9. Kowalczykowski,S.C., Dixon,D.A., Eggleston, A.K., Lauder,S.D., and Rehrauer,W.M. (1994) Biochemistry of homologous recombination in *Escherichia coli*. *Microbiol Rev* 58: 401-465.

10. Krogh,B.O., and Shuman,S. (2002) A poxvirus-like type IB topoisomerase family in bacteria. *Proc Natl Acad Sci U S A* 99: 1853-1858.

11. Levin-Zaidman,S., Englander,J., Shimoni,E., Sharma,A.K., Minton,K.W., and Minsky,A. (2003) Ringlike structure of the *Deinococcus radiodurans* genome: a key to radioresistance? *Science* 299: 254-256.

12. Liu,Y., Zhou,J., Omelchenko,M.V., Beliaev,A.S., Venkateswaran,A., Stair,J. *et al.* (2003) Transcriptome dynamics of *Deinococcus radiodurans* recovering from ionizing radiation. *Proc Natl Acad Sci U S A* 100: 4191-4196.

13. Markillie,L.M., Varnum,S.M., Hradecky,P., and Wong,K.K. (1999) Targeted mutagenesis by duplication insertion in the radioresistant bacterium *Deinococcus radiodurans*: radiation sensitivities of catalase (katA) and superoxide dismutase (sodA) mutants. *J Bacteriol* 181: 666-669.

14. Minton, K.W. (1994) DNA repair in the extremely radioresistant bacterium *Deinococcus radiodurans*. Mol.Microbiol. 13(1):9-15.

15. Misra,H.S., Khairnar,N.P., Barik,A., Indira,P.K., Mohan,H., and Apte,S.K. (2004)

Pyrroloquinoline-quinone: a reactive oxygen species scavenger in bacteria. *FEBS Lett* 578: 26-30.

16. Narumi,I., Satoh,K., Cui,S., Funayama,T., Kitayama,S., and Watanabe,H. (2004) PprA: a novel protein from *Deinococcus radiodurans* that stimulates DNA ligation. *Mol Microbiol* 54: 278-285.

17. Nussenzweig,A., and Nussenzweig,M.C. (2010) Origin of chromosomal translocations in lymphoid cancer. *Cell* 141: 27-38.

18. Rajpurohit,Y.S., Gopalakrishnan,R., and Misra,H.S. (2008) Involvement of a protein kinase activity inducer in DNA double strand break repair and radioresistance of *Deinococcus radiodurans. J Bacteriol* 190: 3948-3954.

19. Rajpurohit,Y.S., and Misra,H.S. (2010) Characterization of a DNA damage-inducible membrane protein kinase from *Deinococcus radiodurans* and its role in bacterial radioresistance and DNA strand break repair. *Mol Microbiol* 77: 1470-1482.

20. Slade,D., Lindner,A.B., Paul,G., and Radman,M. (2009) Recombination and replication in DNA repair of heavily irradiated *Deinococcus radiodurans*. *Cell* 136: 1044-1055.

21. Tian,B., Sun,Z., Xu,Z., Shen,S., Wang,H., and Hua,Y. (2008) Carotenoid 3',4'-desaturase is involved in carotenoid biosynthesis in the radioresistant bacterium *Deinococcus radiodurans*. *Microbiology* 154: 3697-3706.

22. White,O., Eisen,J.A., Heidelberg,J.F., Hickey,E.K., Peterson,J.D., Dodson,R.J. *et al.* (1999) Genome sequence of the radioresistant bacterium *Deinococcus radiodurans* R1. *Science* 286: 1571-1577.

23. Wyman, C., and Kannar, R. (2006) DNA double-strand break repair: all's well that ends well. *Annu Rev Genet* 40:363-383.

24. Zahradka,K., Slade,D., Bailone,A., Sommer,S., Averbeck,D., Petranovic,M. *et al.* (2006) Reassembly of shattered chromosomes in *Deinococcus radiodurans*. *Nature* 443: 569-573.

Packed Fluidization and its Importance in the Development of Fusion Technology

D. Mandal
Materials Section
Chemical Engineering Division
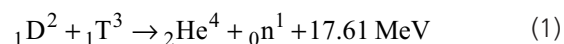*and*
D. Sathiyamoorthy
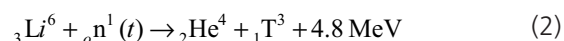Powder Metallurgy Division

Abstract

Experiments were conducted to study heat transfer in unary packed bed and binary packed fluidized bed using lithium titanate and alumina pebbles (size 3-10 mm) and lithium titanate and silica particles (231-780 µm). It was found that due to packed fluidization the rate of heat transfer is enhanced and in terms of the effective thermal conductivity this enhancement was up to 260%. Low thermal conductivity of pebble bed of solid breeder materials is one of the adverse key issues which must be addressed properly for the successful development of the thermonuclear fusion technology. Packed fluidization enhances the effective thermal conductivity of the pebble bed of solid breeder materials in the Test Blanket Module (TBM) of ITER type fusion reactor.

Introduction

Thermonuclear fusion of deuterium and tritium is being considered for the first generation fusion reactors. Significant amount of thermal energy (17.61 MeV) is produced by the fusion of one deuterium (D) and one tritium (T) nucleus as shown in Reaction 1 [1, 2].

$$_1D^2 + {}_1T^3 \rightarrow {}_2He^4 + {}_0n^1 + 17.61\,\text{MeV} \qquad (1)$$

Deuterium (D) is available in nature whereas, tritium is not. Natural hydrogen contains 140 ppm deuterium and the technologies to separate it from the compounds of hydrogen are available, whereas, natural hydrogen contains only 7.0×10^{-12} ppm tritium. Tritium (T) can be produced by irradiation of the Li^6 isotope with thermal neutrons (n (t)) as shown in Reaction 2 [1, 2].

$$_3Li^6 + {}_0n^1\,(t) \rightarrow {}_2He^4 + {}_1T^3 + 4.8\,\text{MeV} \qquad (2)$$

Tritium can't be stored for a long time as its half life is 12.3 years [3]. Lithium (Li)-based ceramics enriched by Li^6 isotope, called solid breeder materials are considered for the generation of tritium for the D-T fusion by ITER (acronym of International Thermo-nuclear Experimental Reactor). Among various compounds of Li, lithium titanate (Li_2TiO_3) and lithium orthosilicate (Li_4SiO_4) are preferred solid breeder materials, because of their chemical and thermal stability, high lithium content and low tritium solubility. These materials will be used in the form of spherical particles (size ≤ 1 mm are called particles and size > 1 mm are called pebbles in this paper) of size 0.8-1.0 mm [1, 2].

Both Li_2TiO_3 and Li_4SiO_4 have low thermal conductivity, which decreases with increase in temperature [4]. Moreover, when spherical particles of these materials are packed in a vessel, cylindrical or rectangular *viz.,* Test Blanket Module (TBM) of ITER type fusion reactor, the effective thermal conductivity (k_{eff}) is further brought down due to the presence of significant amount of voids in the bed. Thus the poor k_{eff} of the particulate bed of these materials is one of the key adverse issues in the fusion technology and it must be enhanced for the successful development of the thermonuclear fusion technology [5].

Li$_2$TiO$_3$ (or Li$_4$SiO$_4$) particles in the TBM will absorb radiation heat from the core of the reactor and heat will also be produced inside the particles during tritium breeding as shown in Reaction 2 [6, 7]. Furthermore, the reaction is exothermic and this warrants the bed to be cooled to favour the tritium breeding. It is considered to purge helium to extract the tritium and also to cool the bed. The extracted tritium must be separated from helium for its use in the fusion. Lesser the concentration of tritium in the extracted gas more will be the separation cost [8, 9].

Dry air was allowed to flow through the unary bed of Li$_2$TiO$_3$ pebbles to study the effect of different process variables on the k_{eff} of unary bed. It was found that the k_{eff} of pebble bed increases with increase in gas velocity at any constant bed wall temperature T_w. But, helium at high flow-rate is not recommended as it will dilute the tritium concentration in the extracted gas. Binary particulate bed has more k_{eff} value than that of unary pebble bed under similar operating conditions [9], but the degree of increase in k_{eff} is not very significant.

The fluidized bed is also not recommended due to the high fluidization velocity (u_{mf}) of Li$_2$TiO$_3$ particles of size 0.8-1.0 mm as they fall under Geldart B class [10-12]. High operating gas velocity (u_o) is not recommended due to dilution of produced tritium in the exit gas. Moreover, in fluidized bed of Li$_2$TiO$_3$ particles, Li density will be very low.

In order to overcome all these aforementioned drawbacks, it is proposed to use packed fluidized bed, where small particles are allowed to be fluidized in the interstitial voids of relatively large and stationary pebbles, called packing [9-12] in the TBM. Packed fluidized bed is a new class of fluidized bed, which can be operated at low gas flow rate and also with low pressure drop across the bed (ΔPb) as compared to the unary bed of large pebbles operating at u_{mf} of small particles. The experimental details and results of studies are discussed in this paper.

Effective Thermal Conductivity of Packed Fluidized Bed

Considering an annulus volume of inner radius r, outer radius r + Δr and height Δz in a cylindrical packed fluidized bed and under some assumptions we can get Equation 3 to predict thermal conductivity ($k_{e,r}$) at any radial location (r) and axial location (z).

$$k_{e,r} = \frac{u_o \left(\rho_g c_p \varepsilon_{pfb} + \rho_p c_{p,f} \varepsilon_p \right) \dfrac{\partial T}{\partial z}}{\left[\dfrac{1}{r} \dfrac{\partial T}{\partial r} + \dfrac{\partial^2 T}{\partial r^2} \right]} \quad (3)$$

where, c_p and $c_{p,f}$ are the heat capacity of gas and small particles, ρ_g and ρ_q are the densities of gas and small particles respectively, ε_{pfb} is the void fraction in packed fluidized bed and T is the temperature at any radial and axial location. [6]

The k_{eff} can be estimated by taking the average of $k_{e,r}$ values at different radial (r) and axial locations (z) which can be measured by finding the radial and axial temperature gradient at different points in the bed by using Equation 3.

Materials and Methods

Materials: Spherical particles of four different sizes *viz.* 231, 427.5, 550 and 780 μm of Li$_2$TiO$_3$ and silica; spherical pebbles of sizes 3, 5, 7 and 10 mm of Li$_2$TiO$_3$ and alumina were used in the study. Li$_2$TiO$_3$ does not occur naturally; neither it is available commercially. Li$_2$TiO$_3$ particles and pebbles used in this study were fabricated by solid state reaction process developed by Mandal *et al.* [1, 2]. Fig. 1 show photographs of some such particles and pebbles. Physical properties of Li$_2$TiO$_3$ particles and pebbles used in the study are reported somewhere else in the literature [12].

Experimental Setup: A schematic diagram of the experimental setup is shown in Fig. 2. The test column was fabricated from a seamless stainless

Fig. 1: Photographs of some Li$_2$TiO$_3$ particles and pebbles used in the experiments, (a) size: 231μm, (b)

Fig. 2: Schematic diagram of the experimental setup, used to study heat transfer in packed and packed fluidized beds.

steel pipe of 163 mm internal diameter and 650-mm height, along with two calming sections. Sandwiched type distributor was used. Dry compressed air was used as fluidizing gas.

Resistance heating wire was used as external heat source. Differential pressure transmitters, on-line gas mass flow meter, several thermocouples and PID controllers were used and the column was insulated. PLC based controller module was used to control gas velocity, heating rate, temperature; data acquisition and storage.

Methods: A known amount of packing pebbles was slowly charged in the test column from the top after removing the upper calming section. Small quantity of packing pebbles at a time was added and arranged them uniformly. Small particles were charged in the column to fill the voids of the packing pebbles and to occupy a known volume percentage (20, 40, 60 and 80) of total void space.

Minimum fluidization velocities of small particles in the interstitial voids of packing pebbles($u_{mf,pf}$) at a given bed wall temperature (T_w) were determined [12].
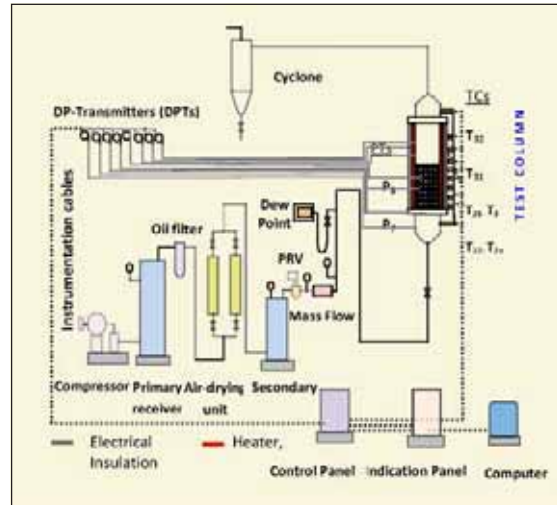
From the temperature profiles the k_{eff} was estimated by taking the average of measured $k_{e,r}$ at four locations using Equation 3. The experiments were repeated with different volume percentage of fluidized particles, bed wall temperatures, sizes of fluidized particles and pebbles, and also with different type particles (Li$_2$TiO$_3$ and silica) and packing materials (Li$_2$TiO$_3$ and Al$_2$O$_3$).

Results and Discussion

Minimum fluidization velocity of small particles in the conventional or unary fluidized bed ($u_{mf,c}$) is the minimum operating superficial air velocity(u_o) at which the pressure drop across the unary fluidized bed (ΔPb) remain constant. Similarly, the minimum fluidized velocity of small particles in packed fluidized bed ($u_{mf,pf}$) is the minimum operating superficial air velocity (u_o) at which the pressure drop across the packed fluidized bed (ΔP_{pfb}) remain constant. $u_{mf,c}$ was measured by plotting ΔPb versus u_o for a unary fluidized bed of small particles and similarly $u_{mf,pf}$ was measured by plotting ΔP_{pfb} versus u_o for a fluidized bed of small particles in binary packed fluidized bed. It was observed that $u_{mf,pf}$ is almost 50% $u_{mf,c}$ of i.e., the minimum fluidization

velocity of small particles in unary fluidized bed is reduced by almost 50% in the packed fluidized bed [12]. Based on the experimental results a correlation (Equation4) has been developed to estimate minimum fluidization velocity of small particles in packed fluidized bed ($u_{mf,pf}$).

$$\frac{u_{mf,pf}}{u_{mf,c}} = 153.28 \times 10^{-2} \frac{\varepsilon_P}{X_f^{0.1}} \left[\frac{\mu_a}{\mu_{T_w}}\right]^{0.6} \left[\frac{\rho_{g_{T_w}}}{\rho_{g_{T_a}}}\right]^{0.25} \qquad (4)$$

where, ε_p is the void fraction of pebble bed, X_{fi} is the volume fraction of small particles in the interstitial void volume of packing pebbles, μ_a and μ_{T_w} are the viscosity of air at ambient and bed wall temperature T_w, respectively, ρ_{ga} and ρ_{gTw} are the density of gas at ambient temperature and T_w, respectively. Subscripts T_a and T_w indicate ambient and wall temperatures, respectively.

Temperature Gradients: Due to fluidization of small particles, temperatures at all locations in packed fluidized bed were higher than the corresponding locations in packed bed as shown in Figs. 3 (a) and (b). Voids in the packed beds offer higher resistance to heat transfer than the pebble material; this resistance is lowered significantly when small particles are fluidized and enhance heat transfer in the voids.

Effect of Operating Gas Velocity: Fig. 4 shows how k_{eff} of packed fluidized bed($k_{eff,pfb}$) changes with the operating velocity ratio($u_o/u_{mf,pf}$), bed wall temperature(T_w) and when small particles occupy 20 % of the volume($X_{fi}=0.2$) of the voids and 60 % of the volume. It was found that increases with decrease in particle to pebble size ratio(d_p/D_p) at different bed wall temperature and also for different materials.

The beds were operated at four operating gas velocities $u_{mf,pf}$, $2u_{mf,pf}$, $3u_{mf,pf}$, and $4u_{mf,pf}$. As the operating gas velocity ratio ($u_o/u_{mf,pf}$) exceeds 1, particles in the voids are fluidized, start colliding with the packing and themselves more frequently and thus improve heat transfer rates. At $u_o/u_{mf,pf} > 3$, the particles are carried over to the top of the bed and therefore reduce their fraction in the voids of the bed. This carryover leads to a decrease in k_{eff} of the bed.

Effect of Filling of Small Particles in Interstitial Voids: It was observed that ($k_{eff,pfb}$) increases with increase in volume % of filling of voids with particles as shown in Fig. 4a (for 20 volume %) and Fig. 4b (for 60 volume %). That is a higher can be obtained when 60 volume % of voids are filled with smaller particles. For 60 volume
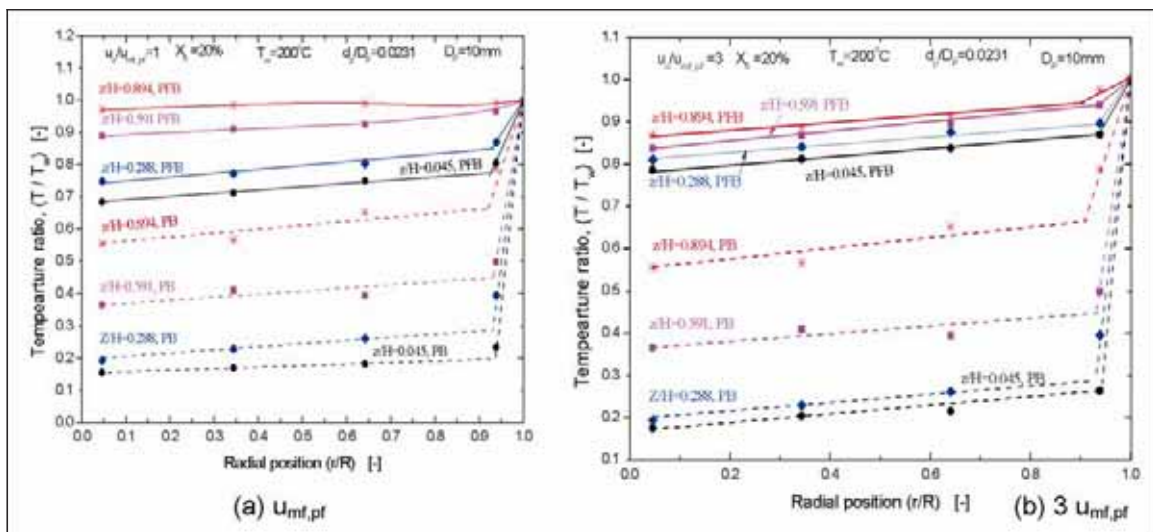

Fig. 3: Radial temperature profiles of packed fluidized bed (in solid lines) of 20 volume percent 231μm particles in the interstitial void volume of 10 mm Li$_2$TiO$_3$ pebbles at bed wall temperature 200°C at (a) $u_{mf,pf}$ (b) 3 $u_{mf,pf}$.

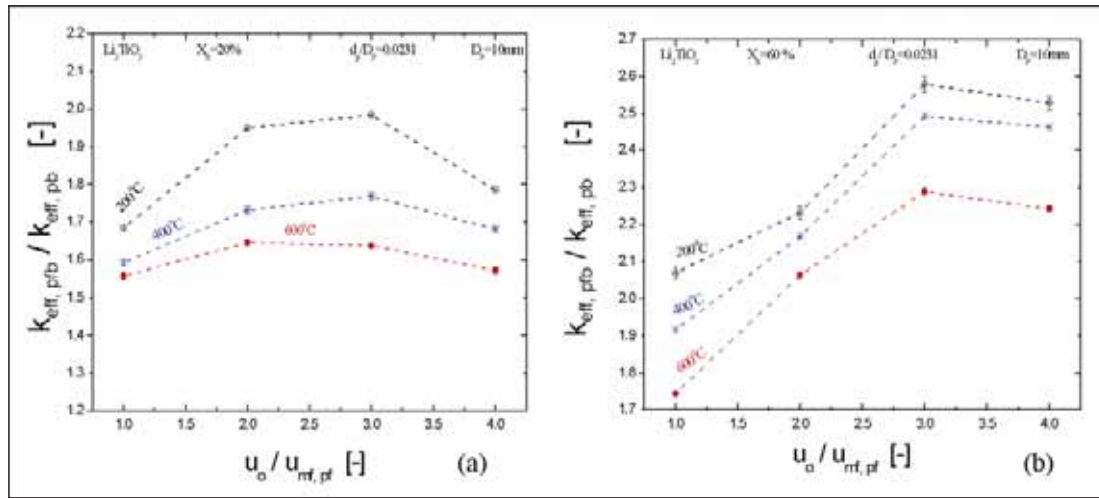Fig. 4: Variation of effective thermal conductivity of packed fluidized bed of (a) 20 volume % and (b) 60 volume % fluidized Li_2TiO_3 particles of particle size 231μm (d_p) in the interstitial void volume of 10 mm Li_2TiO_3 particles with operating gas velocity ratio ($u_o/u_{mf,pf}$)

% filling of voids, values in a packed fluidized bed increased up to 1.97 Wm^{-1} K^{-1} at 200°C bed wall temperature, which is close to the thermal conductivity of Li_2TiO_3 pebble at 200°C (2.1 Wm^{-1} K^{-1}).

Effective Thermal Conductivity

A correlation (Equation 5) to evaluate effective thermal conductivity of packed bed (k_{eff}) has been developed, tested with experimental results and found to have good agreement with our model prediction. The developed correlation for estimating k_{eff} in packed bed is:

where, $k_{a,T}$ is the thermal conductivity of air at ambient temperature T_a, k_{eff} is the effective thermal conductivity of Li_2TiO_3 pebble bed at bed wall temperature T_w is the bed wall temperature and Re$_p$

$$\frac{k_{eff}}{k_{a,T}} = 18\,\mathrm{Re}_p^{0.2}\left(\frac{T_w}{T_a}\right)^{-0.14} \quad for \quad \mathrm{Re}_p < 15) \quad \text{and}$$

$$\frac{k_{eff}}{k_{a,T}} = 15\,\mathrm{Re}_p^{0.2}\left(\frac{T_w}{T_a}\right)^{-0.44} \quad for \quad \mathrm{Re}\,p \geq 15 \quad (5)$$

is the particle Reynolds number to be evaluated using uo at T_a and gas properties at T_w. Variation of k_{eff} with void fraction in unary and binary particulate bed was recently studied by Mandal et al. [13].

Based on the experimental results a correlation (Equation 6) has been developed to estimate effective thermal conductivity of packed fluidized bed from thermal conductivity of gas(k_g) and solid (k_s), volume fraction of small particles in the interstitial voids(X_{fi}), void fraction of bed (ε_{pfb}),

$$\frac{k_{eff,pfb}}{k_g} = \frac{k_s}{k_g}(1-\varepsilon_{pfb}) + 7.7\mathrm{x}10^{-2}\,X_{fi}^{0.15}Pe^{0.33}\left(\frac{D_P}{d_p}\right)^{1.1} \quad (6)$$

Peclet number (Pe) and size ratio of small particles to packing particles(D_p/d_p) [14].

Conclusions

Studies in packed fluidized bed on heat transfer reveal that enhancement of the effective thermal conductivity is up to 260% and it need low gas velocity since minimum fluidization velocity of particles in packed fluidized bed is about 50% of that in unary fluidized bed. The packed fluidization technique is well applicable to the fusion technology due its many advantages. Due to the presence of

small particles in the interstitial voids of packing the effective thermal conductivity is enhanced. Moreover, due to the addition of small particles in the interstices of pebbles, the overall bed density is increased, which is very useful for TBM, where higher packing density and higher heat transfer rates are essential at low gas velocities. This packed fluidization will play an important role in fusion technology.

Nomenclature

Symbols

c_p	heat capacity, suffix p for gas and p, f for fluidized particles $[Jkg^{-1}K^{-1}]$
d_p	diameter of small particles [m]
D_p	diameter of packing pebbles [m]
k_{eff}	effective thermal conductivity of pebble bed $[Wm^{-1}K^{-1}]$
$k_{eff,pb}$	effective thermal conductivity of packed pebble bed $[Wm^{-1}K^{-1}]$
$k_{eff,pfb}$	effective thermal conductivity of packed fluidized bed $[Wm^{-1}K^{-1}]$
$k_{e,r}$	effective thermal conductivity of pebble bed at radial position r $[Wm^{-1}K^{-1}]$
r	radius of bed [m]
T	Temperature, suffix g for gas, a for ambient and w for that at bed wall [K]
u_o	operating superficial gas velocity $[ms^{-1}]$
u_{mf}	minimum fluidization velocity, (bases on superficial gas velocity) $[ms^{-1}]$
$u_{mf,c}$	minimum fluidization velocity (bases on superficial gas velocity) of small particles in conventional fluidized bed i.e., in absence of packing $[ms^{-1}]$
$u_{mf,pf}$	minimum fluidization velocity in packed fluidized bed, $[ms^{-1}]$
X_{fi}	volume fraction of particles in the interstitial void volume of pebbles [-]
z	axial height [m]

Greek letters

ΔP_b	pressure drop across the unary fluidized bed $[Nm^{-2}]$
ΔP_{pfb}	pressure drop across the binary packed fluidized bed $[Nm^{-2}]$
ε	void fraction, suffix p for packed bed (i.e. in absence of particles), pfb for packed fluidized bed, mf for value at minimum fluidization velocity [-]
μ	viscosity of gas, suffix T_a for that at ambient and T_w for that at bed wall temperature $[kg\ m^{-1}s^{-1}]$
ϕ_S	particle sphericity [-]
ρ_g	density of gas, suffix p in place of g for fluidized particles $[kgm^{-3}]$

References

1. Mandal D., Shenoi M. R. K., Ghosh S. K., Synthesis and Fabrication of Lithium-titanate Pebbles for ITER Breeding Blanket by Solid Phase Reaction and Spherodization, *Fusion Eng. Des.*, 85, 819-823, 2010.

2. Mandal D., Sathiyamoorthy D., Rao V. G., Preparation and Characterization of Lithium-Titanate Pebbles by Solid-State Reaction and Spherodization Techniques for Fusion Reactor, *Fusion Eng. Des.* 87, 7-12, 2012.

3. Mandal D., Sen D., Mazumder S., Shenoi M. R. K., Ramnathan S., Sathiyamoorthy D., Sintering Behaviour of Lithium-Titanate Pebbles: Modifications of Microstructure and Pore Morphology, Mechanical Properties and Performance of Engineering Ceramics and Composites VI, Volume 32, John Wiley & Sons, Inc., Hoboken, NJ, USA., 2011.

4. Mandal D., Sathiyamoorthy D., Vinjamur M., Experimental Measurement of Effective Thermal Conductivity of Packed Lithium-Titanate Pebble Bed, *Fusion Eng. Des*, 87, 67-76, 2012.

5. Mandal D., Sathiyamoorthy D., Vinjamur M., Heat Transfer Characteristics of Lithium-Titanate Particles in Gas-Solid Packed Fluidized Bed, *Fusion Sci. Technol*, 62(1), 150-156, 2012.

6. Dalle D. M., Sordon G., Heat Transfer in Pebble Beds For Fusion Blankets, *Fusion Tech.*, 17, 111-115, 1990.

7. Sullivan J., Canadian Ceramic Breeder Sphere Technology-Capability and Recent Results, *Fusion Eng. Des.*, 17, 79-85, 1991.

8. Donne M. D., Goraieb A., Piazza G., Sordon G., Measurements of the effective thermal conductivity of a Li_4SiO_4 pebble bed, *Fusion Eng. Des*. 49–50, 513–519, 2000.

9. Mandal D., Sathiyamoorthy D., Khakhar D. V., Fluidization Characteristics of Lithium-titanate in Gas-Solid Fluidized Bed, *Fusion Eng. Des.*, 86, 393-398, 2011.

10. Sutherland J.P., Vassilatos G., Kubota H., Osberg G. L., The Effect of Packing on a Fluidized Bed, *AIChE J.*, 9 (4), 437-441, 1963.

11. Zeigler e N., Brazelton W.T., Radial Heat Transfer in Packed-Fluidized Bed, *Ind. Eng. Chem. Proc. Des. Dev.*, 2(4), 276-281, 1963.

12. Mandal D., Sathiyamoorthy D., Vinjamur M., Hydrodynamics of Beds of Small Particles in the Voids of Coarse Particles, *Powder Technol.*, 235, 256–262, 2013.

13. Mandal D., Sathiyamoorthy D., Vinjamur M., Void fraction and effective thermal conductivity of binary particulate bed, *Fusion Eng. Des*, 88, 216-225, 2013.

14. Mandal D., D., Sathiyamoorthy D., Vinjamur M., Experimental Investigation of Heat Transfer in Gas-Solid Packed Fluidized Bed, *Powder Technol.*, 246, 252–268, 2013.

Development and Validation of Methodology for Dryout Modeling in BWR Fuel Assemblies and Application to AHWR Design

D. K. Chandraker, A. K. Nayak and P. K. Vijayan
Reactor Design and Development Group

Abstract

Critical Heat Flux (CHF) is a vital parameter for the thermal design of a fuel bundle and the existing approaches are not reliable owing to its strong dependency on the geometrical and operating parameters. In addition, the approaches for the rod bundles are proprietary owing to the expensive experimentation and technical challenges associated with simulation of nuclear heating for a prototype rod bundle. In view of this, a methodology for the modelling of the CHF phenomenon under BWR operating conditions has been developed and validated in BARC. The phenomenon of the liquid film flow and associated deposition and entrainment of droplets in annular flow regime has been considered to carryout dryout modelling in conjunction with the subchannel analysis. The proposed methodology has been found to provide excellent prediction when compared with the critical power data of rod bundles for different configurations. Using the validated methodology, the critical power (thermal margin) for a new design of AHWR fuel assembly has been evaluated. The available thermal margin indicates potential for uprating of AHWR power. Development of the proposed methodology for the dryout modelling provides excellent prediction of thermal margins for BWR fuel assembly.

Introduction

Critical Heat Flux (CHF) is the maximum heat flux beyond which the surface temperature rises sharply (Fig. 1) and corresponding limiting power is called the critical power which is an important consideration for the thermal design of nuclear fuel bundle. CHF was first discovered by Nukiyama in 1934 and subsequently it is regarded as an important design parameter for thermal systems, most importantly, nuclear reactors. The nuclear fuel bundle must be operated well below the CHF to ensure adequate thermal margin required for operating flexibility and to account for uncertainties in the prediction of CHF. Enormous amount of CHF data has been generated in the past and around 1000 empirical correlations exists which is due to the underlying complex mechanisms. The CHF experiments on the prototype bundle is cost intensive due to very high power requirement and technologically challenging in terms of simulation of nuclear heating having axially and radially varying power profiles. Evaluation of CHF is a must for
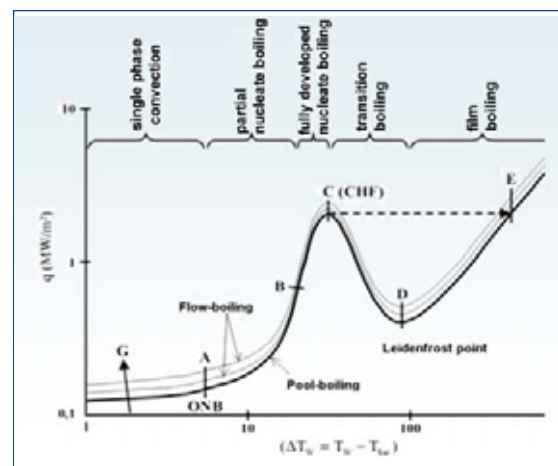

Fig. 1: Nukiyama Curve for CHF (heat flux vs. wall superheat)

licensing of a reactor having new fuel design. Under the BWR conditions (high quality), CHF is caused due to the progressive depletion of the liquid film over the heated surface (Fig. 2). This phenomenon is generally referred to as Liquid Film Dryout (LFD). The phenomenological (mechanistic) models for LFD have been suggested by various investigators and

over the years leading to a considerable improvement in the mechanistic prediction of dryout.

Due to the above consideration, mechanistic modeling of the CHF phenomenon has gained momentum among the thermal hydraulic community with varying level of success. In a simple geometry the mechanistic modeling approach of dryout is found to provide encouraging prediction but there are limited validations under the reactor conditions. Also, the treatment of the mass transfer process at the liquid film and vapor interface has been understood quite well but the validation under the BWR conditions is scarce owing to limited experiments on the measurement of liquid film flow rate in annular steam-water conditions. Thus validation of the approach for entrainment and deposition process is necessary which has been done in the present study as a first step for modeling the phenomenon in the complex geometry such as the rod bundle. The method of dryout modeling in the rod bundle has been proprietary and hence reliable information on the details of modeling process is inadequate. Secondly, the treatment of film flow around the rod due to the subchannel effect has also not been recommended in the literature as the film flow mixing is very complex across the subchannels.

In view of above consideration, in the present work, a methodology has been developed and validated for the critical power prediction in BWR fuel assemblies using phenomenological approach. The dryout modeling is initially developed for a single channel (tube) and entrainment and deposition approach was validated using the experimental data of BARC generated under BWR operating conditions. Subsequently, the approach is applied to the rod bundle considering subchannel interaction and liquid film flow in various rods. The present work details out the development of methodology for the dryout modeling in rod bundle. A computer code, FIDOM-Rod has been developed and validated using the critical power test data for 16, 19 and 37
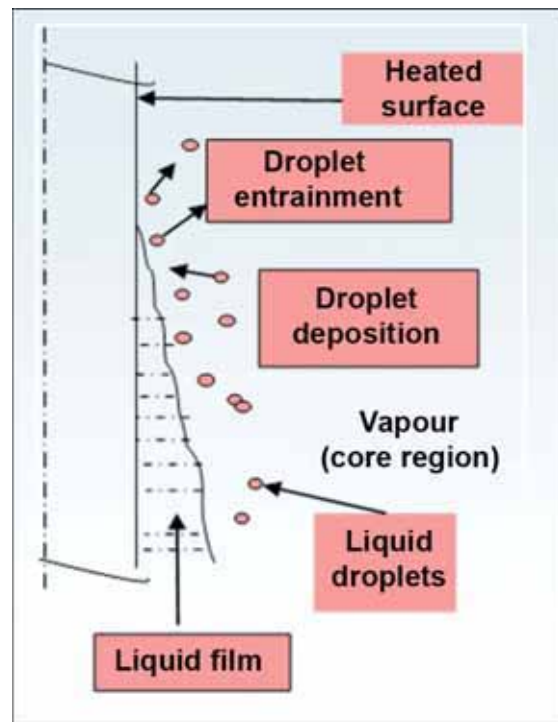

Fig. 2: Progressive depletion of the liquid film and three fluid steams (liquid film, droplets and vapor core)

rod bundles. Finally critical power of untested bundle of AHWR has been evaluated using FIDOM-Rod.

Liquid Film Dryout Modeling in a Rod Bundle

The LFD in an annular two phase regime relevant to BWR operating conditions (high quality) involves treatment of interface mass transfer of droplets due to entrainment and deposition (Fig 2). Progressive depletion of the liquid film due to the mass transfer results into dryout conditions and corresponding heat flux is called critical heat flux which is a vital parameter to evaluate the maximum power that can be derived from a given fuel design.

In the liquid film analysis, the conservation equations of mass and energy for the liquid film, entrained droplets and vapor are solved. Since the film dryout modeling for a rod bundle utilizes the subchannel information derived from the subchannel code (e.g. COBRA), certain assumptions are required to be made to simplify the analysis as given below.

- Each subchannel is assumed to behave like a tube considering cross flow and mixing as is done in the subchannel analysis.
- The mass flux, quality and the exchange of liquid and vapour between the subchannels is dictated by subchannel formulation.
- As the total liquid flow rate in the subchannel comprises the film flow rate and droplet flow rate, the droplet content in the vapour core changes axially depending on the deposition rate (m_d), entrainment rate (m_e) and film evaporation rate (m_{ev}) in the subchannel.
- The fuel rod experiences different entrainment and deposition rates circumferentially as it is facing different subchannel conditions (Fig. 3). The process of exchange of liquid film around the rod is a complex phenomenon and there is a strong tendency to achieve uniformity in the film flow rate due to the inter-channel cross flow in the circumferential direction. Hence, in the present analysis it is made uniform before proceeding to the next node.
- The dryout is initiated when the liquid film vanishes on any one the rods.

The important aspects of the modeling are the mass exchange at the interface between the liquid film and the vapour core region (Fig. 2).

Mass balance (w_{lf}) of the liquid film (k) in a subchannel is given by

$$\frac{dw_{lf}^k}{dz} = P^k \left(m_d - m_e - m_{ev} \right)_k + \frac{dw_{lf\_cf}^k}{dz} \qquad (1)$$

Liquid film mass conservation (w_{sclf}) for the subchannel having 'n' liquid films (susbsript "cf" refers to the cross flow components)

$$\frac{dw_{sclf}}{dz} = \sum_{k=1}^{n} P^k \left(m_d - m_e - m_{ev} \right)_k + \frac{dw_{sclf\_cf}}{dz} \qquad (2)$$

For the droplets in a subchannel (w_{scld}) surrounded by 'n' number of liquid films

$$\frac{dw_{scld}}{dz} = \sum_{k=1}^{n} P^k \left(m_e - m_d \right)_k + \frac{dw_{scld\_cf}}{dz} \qquad (3)$$

Total liquid flow composed of liquid film and droplets is computed by Subchannel Analysis Module (SCAM) as given by following equation

$$\frac{dw_{scl}}{dz} = \frac{dw_{sclf}}{dz} + \frac{dw_{scld}}{dz} \qquad (4)$$

Hence

$$\frac{dw_{scld}}{dz} = \frac{dw_{scl}}{dz} - \frac{dw_{sclf}}{dz}$$

Thus the droplet flow rate in a subchannel is the difference between the total liquid flow (by subchannel code) and the film flow rate (evaluated by LFD module).

Energy balance in a given subchannel is

$$m_{ev} = \sum_{k=1}^{n} \frac{q_k}{h_{fg}} \qquad (5)$$

After calculating the film flow rate in the rod surfaces for all the subchannels, the film flow rate around any rod is averaged circumferentially at each axial location before proceeding for the analysis for the next node. Thus film flow rate is averaged considering 'l' number of liquid film around the rod as given below.

$$\left(w_{lf}^k \right)_{updated} = \frac{w_{rlf} P^k}{\sum_{k=1}^{n} P^k} ...and \quad w_{rlf} = \sum_{k=1}^{l} w_{lf}^k$$

Where, $(w_{lf}^k)_{updated}$ is the updated value of film flow rate in the surface (k) of the rod.

The mass transfer correlations for the entrainment and deposition of the liquid droplets proposed by Whalley are given below.

$$m_e = KC_{eq} \text{ and } (m_d = KC)$$

Where K is the mass transfer coefficient and C is the droplet concentration prevailing in subchannel. C_{eq} is the liquid concentration at equilibrium which is related to the entrainment.
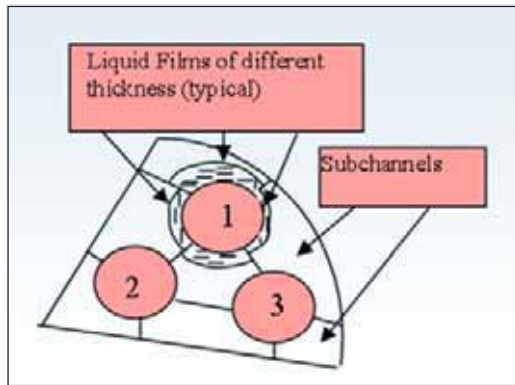
Fig. 3: Typical formation of liquid film on the rod surfaces facing different subchannels

The droplet mass per unit volume is given by

$$C = \frac{\rho_l\, j_{ld}}{j_g + j_{ld}} = \frac{\rho_l\, j_l E}{j_g + j_l{}^i}$$

Where j_g and j_l are the superficial velocities for the gas and liquid droplets in the subchannel respectively. E is the entrainment fraction defined as the ratio of the entrained liquid droplets to the total liquid in the subchannel. Utsuno and Kaminaga's models for the entrainment fraction at equilibrium (Eeq) and deposition coefficient (K), in the BWR operating range have been considered following their validation with BARC data.

$$E_{eq} = \tanh\left(0.16 W_e^{0.08}\, R_{el}^{0.16} - 1.2\right) \tag{6}$$

$$K = 41.2 \frac{\mu_g}{\rho_g D} Re_g^{0.15} \left(\frac{c}{\rho_g}\right)^{-0.36} \tag{7}$$

The initial entrainment fraction right after the transition to the annular-mist flow is assumed to be at equilibrium.

The code, FIDOM-Rod has been developed to perform the dryout calculation in the rod bundles and it interfaces with the subchannel analysis module (SCAM) module to evaluate the local mass flux and quality

Interfacing with the subchannel code

At first, the subchannel analysis is performed for a given assembly power using SCAM. The subchannel enthalpy and mass flux are the input to the LFD

Analysis Module (LFDAM). The location of the onset of droplet entrainment is determined for each subchannel which is the starting point for the progression of the liquid film.

Once the annular flow sets in for all the subchannels facing the rod under consideration, the dryout analysis is triggered for this rod. Thus the code of LFDAM module (FIDOM-Rod) analyses each film in the subchannels considering different entrainment rate, deposition rate evaporation rate depending upon the rod power peaking. Once the flow rate of each film is analyzed swiping over the entire cross section, the liquid film flow rate around the rod at any axial location is made uniform circumferentially. The channel power is increased till the dryout condition is achieved (Fig. 4).

Validation of the models of entrainment and deposition rates using BARC data

Experiments have been carried out in BARC in a single channel geometry having heated length of 3.5 m and the inner diameter of 8.8 mm. A total of 125 data points have been generated in the present
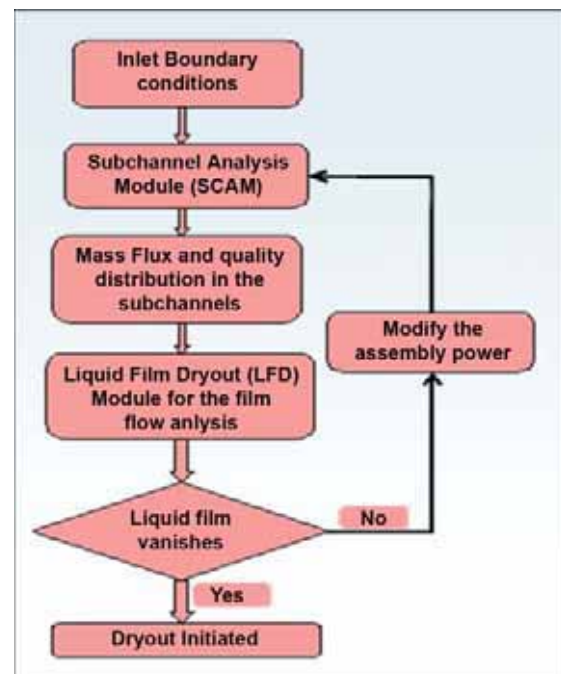

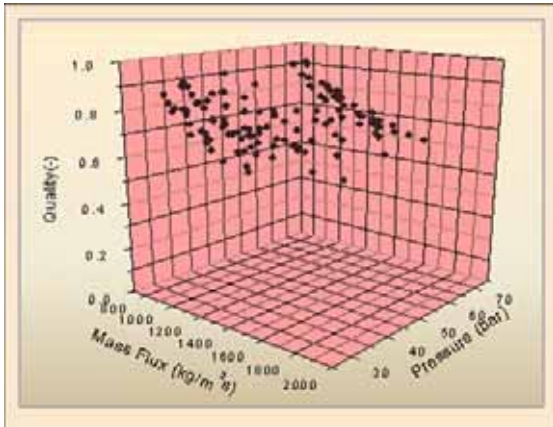Fig. 4: Interface between the liquid film dryout and subchannel analysis modules

Fig. 5: Operating range of experimental
data of BARC

Fig. 7: Comparison between the CHF prediction by
Mechanistic approach and the Experiment

phase of CHF experiments. The experimental range (Fig. 5) of the operating conditions is as given below. Inlet Pressure: 29 - 71.4 (bar), Mass Flux: 803.1-1912.6 (kg/m²s), Exit quality: 0.468-0.964, Inlet subcooling : 6.2-61.7 °C, Heat flux : 832 to 1220 kW/m². These ranges correspond to AHWR operating conditions.

Fig. 6 shows the geometry of the test section and location of the thermocouples for CHF detection. Fig. 7 shows the comparison of the prediction and experimental values of CHF. The results show that the phenomenological prediction is made within the error band of ±10%. Out of 125 data points around 83 data predicted within ± 5%. The prediction within this error band is excellent as compared to the empirical approaches having limited range of validity. Thus the present investigation substantiates the validity of the models adopted in the phenomenological approach under
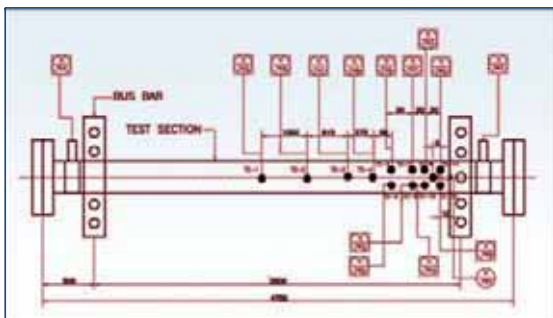
BWR condition. Other models of entrainment and deposition rates are found to provide prediction beyond ±30%. Hence validation of the models is necessary before applying to the rod bundle.

Validation of the Rod bundle dryout modeling approach (FIDOM-Rod)

The mechanistic tool, FIDOM-Rod was developed to perform dryout analysis in the 16, 37 and 19 rod bundle and compared with the experimental data available in the open literature. The Range of the parameters for the data is given in Table 1. Configurations for the 16 and 37 rod bundles are shown in Figs. 8 and 9 respectively. Thus, FIDOM-Rod prediction has been compared with the dryout data of rod bundles having different configurations and peaking factors

Table 1: Rod bundle data on dryout for validation of dryout modeling approach

No. of Rods	: 16, 19 and 37
No. of data	: 63
Pressure (bar)	: 68-102
Mass flux (kg/m2s)	: 485-2712
Inlet subcooling (°C):	227.41°C-39.3% quality
Dryout quality(-)	: 0.212-0.686
Dryout power	: 0.837-5.358 (MW)

Variation of droplet and film parameters for 16 rod bundle

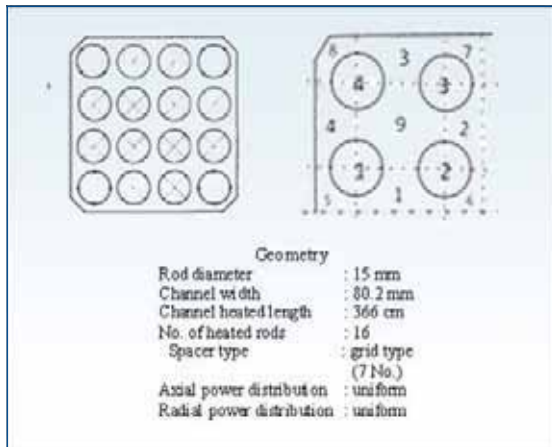Figs. 10 and 11 shows the important parameters like the entrainment fraction (E) in subchannels, and

Fig. 6: Test section used and thermocouple locations in CHF experiments

Fig. 8: 16 rod bundle cross section and ¼ symmetry sector
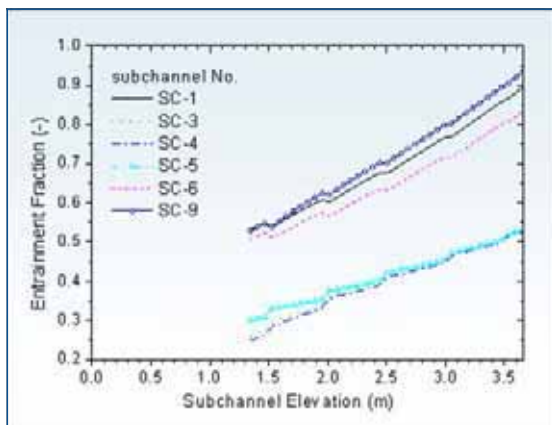

Fig. 11: Film flow rate in the 16 rod bundle

film flow rates in the rods. It can be seen that the entrainment fraction is higher for the inner subchannels (1, 6, 9 in the plot) and tends to be less in the side and corner subchannels (3, 4, 5 in the plot) which can be attributed to the presence of unheated wall in the side and corner subchannels causing film flow to be higher in absence of any evaporation.

Fig. 11 depicts the variation of film flow rate for each rod at the dryout condition. The dryout is found to get initiated in the critical rod (rod no. 3) due to complete vanishing of the liquid film.

Variation of Critical Power with the Subcooling and Mass flow rate

The trend of critical power with the subcooling for different mass flux (500, 1000, 1500 and 2000 kg/m²s) is depicted in fig. 11 and compared with the mechanistic prediction of FIDOM-Rod for 16 rod bundle.

Comparison with dryout data of 16 rod, 19 rod and 37 rod bundles

Fig. 13 shows the comparison between the model prediction and experimental data for 16, 19 and 37 rod bundles having different configurations. It can be seen that most of the data is predicted with deviations within ±10%. However, the deviation is higher for the case having low dryout quality (due to very high flow rate and/or high subcooling).
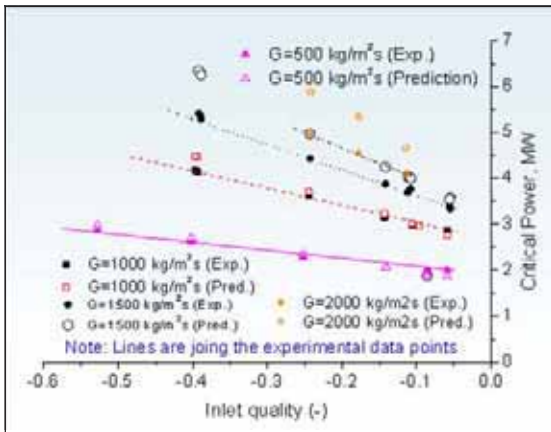

Fig. 9: 37 Rod configuration and 1/6 Symmetry sector

Fig.10: Entrainment fraction in the subchannels of 16 rod bundle

Fig. 12: Measured and predicted critical power with the inlet subcooling (16 rod bundle)

Fig. 13: Experimental data and model

In the present analysis the dryout power below 0.25% quality is predicted within ± to 20% accuracy. In the operating BWRs the normal operating quality is around 25% but the dryout quality is much higher (above 40%) depending upon the mass flux and inlet condition. The LFD model is applicable for the higher dryout quality in the annular flow region (BWR range).

Thus FIDOM-Rod prediction is found to be within ±10% under the BWR operating range.

Model for Spacer Effect on Deposition

The spacer is a vital component in nuclear fuel rod assembly to maintain appropriate gap between the rods allowing coolant to perform its assigned function. A large amount of test data is required for the optimum design of the spacer in absence of the mechanistic modeling of the spacer. Hence the development of a model for the spacer based on the study of the flow behavior downstream of the spacer is an important aspect of the LFD analysis. The literature review on the spacer effect in BWR assemblies indicates that the droplet deposition is generally enhanced downstream of the fuel spacer because of change in the velocity profiles in the narrow passage and wider passage at the spacer location. The process of velocity recovery downstream of the spacers results into the lateral velocity components causing liquid droplets to transport on the fuel rod (drift velocity
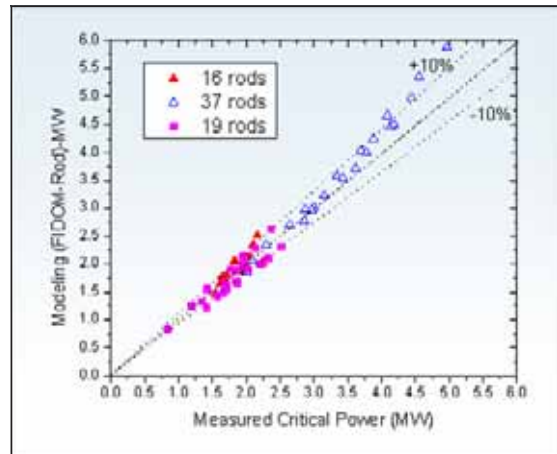
phenomenon). In addition, the liquid film is deposited on the spacer wall also which gets dislodged at the spacer edge and joins the core flow affecting the film flow on the rods (run-off effects). The liquid film flow on the rod is obstructed at the spacer location (narrow channel effect). Thus, drift velocity, run-off effect and narrow channel effects are three major mechanisms to be considered for the deposition of the droplets in BWR assemblies. To consider the spacer effect in AHWR, the turbulence enhancement factor is defined as

$$= \text{TKE} = \frac{Kinetic\ energy\ with\ spacer}{Kinetic\ energy\ without\ spacer}$$

The CFD analysis of AHWR spacer (Fig. 14) for a gas phase indicated that this factor is independent of the gas velocity and a model has been provided considering assumed distance of 50 mm from the spacer for attaining the peak value of TKE (Fig. 15) based on investigation by researchers. This model is plugged into FIDOM-Rod to account for the spacer effect.

Critical power evaluation for 54 rod bundle of AHWR

Subsequent to the validation of the dryout methodology (FIDOM-rod), the prediction of critical power for the untested 54 rod cluster of AHWR (Fig. 16) has been carried out. A simple spacer model proposed for AHWR spacer has also been developed to quantity its effect on the thermal margin. Fig. 17
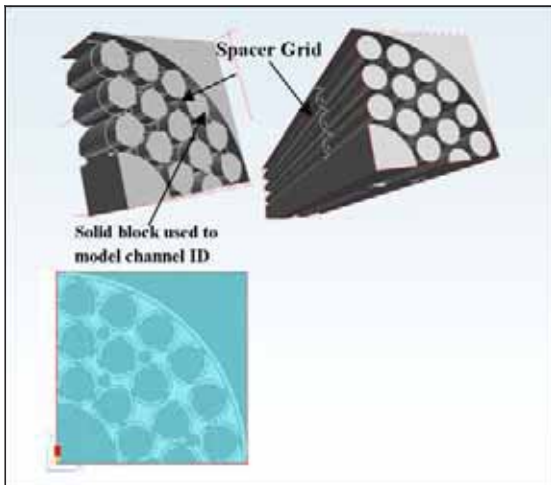
Fig. 14: ¼th symmetry sector of AHWR fuel cluster considered for analysis   (the spacer grid, assembly of spacer and rod cluster and 90 x 90 computational grid across the cross section
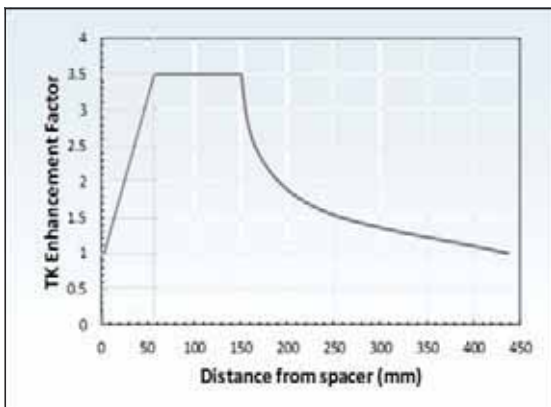

Fig. 15: Proposed spacer model of 54 AHWR bundle evaluated using CFD analysis
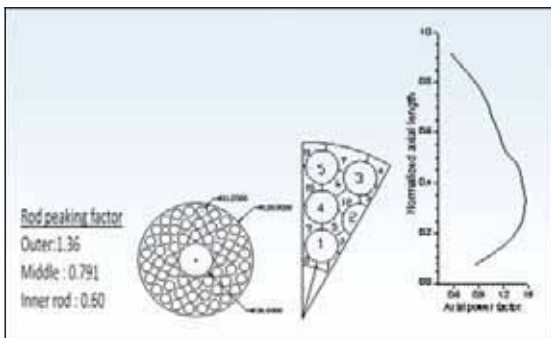

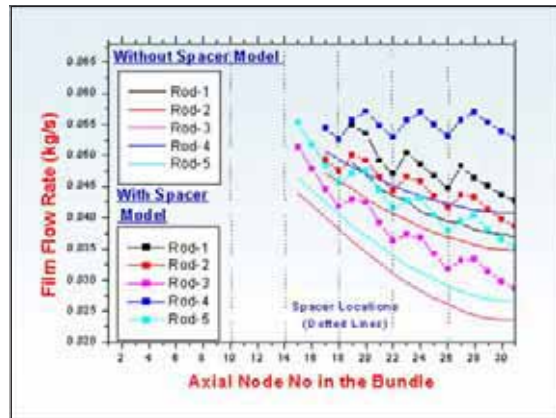Fig. 16: Schematic of 54 fuel pin Rod bundle of AHWR, 1/12th symmetrical sector and axial power profile

Fig. 17: Film flow rate in the rods of 54 rod cluster of AHWR

depicts the film flow rates on the rods at 150% power corresponding to 70 bar and 1000 kg/m²s. The effect of spacer on the rod film flow rate is also shown for comparison. The rod 2 has minimum film flow rate and is the critical rod (having maximum rod peaking of 1.36) from dryout consideration.

Fig. 18 depicts the variation of Critical Power Ratio (CPR) with mass flux at operating pressure of 70 bar and subcooling of 25 ºC. The trend of CPR indicates that the critical power of a bundle increases with the mass flux.

The mass flux of the bundle reduces with the reactor power Fig. 18 shows the reduction in the channel flow rate also as the power is increased. The interaction of these two graphs indicates the operating point at the critical power of the bundle. The critical power ratio the bundle has been determined to be 1.51 with the spacer effect. Fig. 19 shows that adequate thermal margin exists during the reactor start up when the channel power is raised to the normal power during start-up of the reactor.

Thus the present validated methodology provides provides the thermal margin of untested 54 rod bundle of AHWR.

Conclusions

In this research, a mechanistic tool (FIDOM-Rod) for the dryout modeling of BWR assemblies have been developed, validated and applied to AHWR
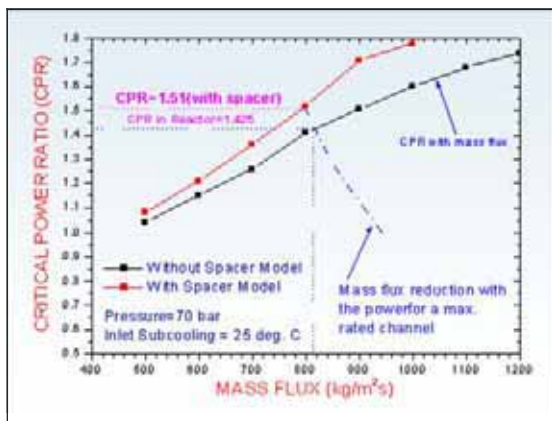
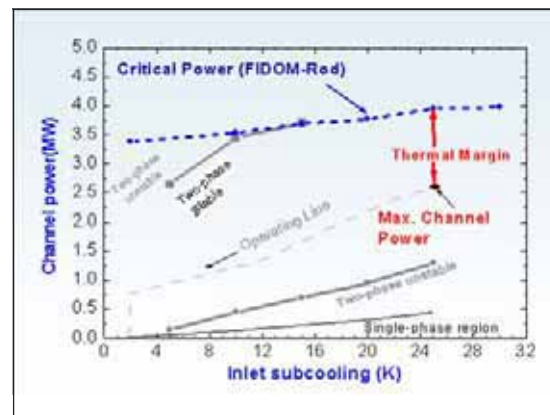Fig.18: Critical power of AHWR with mass fluxes

Fig. 19: Critical channel power for AHWR showing the steady state operating line and stable zone of operation

design for the evaluation of thermal margins. The following conclusions have been made in the present work.

1) The proposed phenomenological modeling of dryout has potential to replace the existing CHF correlations for rod bundle (usually proprietary in nature and vender specific) due to excellent prediction for BWR rod assemblies within ±10%. It may be noted that

2) The validation of methodology adopted in the code, FIDOM-Rod confirms that uniform liquid film flow rate around the rod is justified for the dryout modeling in the rod bundles. The validation of such approach is limited in the literature.

3) The deposition model and entrainment model selected for the CHF in tube has also been found to be adequate when compared with BARC data.

4) The methodology, FIDOM-Rod has been applied to the untested 54 rod bundle of AHWR and the critical power ratio has been evaluated to be 1.51 while accounting for the spacer effect. It may be noted that the existing empirical approaches are highly unreliable/conservative due to the strong geometrical dependency of CHF and the proposed methodology is expected to provide excellent prediction accuracy for the untested bundle of AHWR.

6) The critical power approach indicates absolute power margin available in the bundle. Considering the margins available (51%), there is a possibility of power uprating of AHWR. This will be further explored in the full scale dryout experiments in AHWR Thermal Hydraulic Test Facility (ATTF) being set-up at R&D Centre, Tarapur.

7) Since the FIDOM-Rod predicts the critical power with significantly good accuracy for the BWR rod assemblies, this methodology can be used to optimize the rod bundle configuration, local and axial peaking factors for enhancing the critical power. Hence the thermal margins available in the fuel assemblies can be ascertained with excellent accuracy using the methodology of FIDOM-Rod developed in BARC.

Acknowledgement

Development of Radiological Monitoring Systems & Techniques for Operations, Process safety and Decommissioning

R.K.Gopalakrishnan, K.S.Babu, S.Priya, D.P.Rath, Sanjay Singh, P. Srinivasan, M.K. Sureshkumar, K.S. PradeepKumar and D.N.Sharma
Radiation Hazards Control Section
Radiation Safety Systems Division

Abstract

The Radiation Hazards Control (RHC) Section of the Radiation Safety Systems Division (RSSD) provides safety coverage on radiological aspects to various plants and facilities of BARC and other DAE units. The Division extends its expertise in dealing with safety matters pertaining to design, commissioning and operation of nuclear facilities. This report briefly summarizes the routine and the major developmental activities carried out by the various RHC units.

Introduction

Several nuclear and radiation handling facilities encompassing all the stages of nuclear fuel cycle and radiation applications are located in BARC, Trombay. Radiological Safety Officers (RSOs) and professionally trained health physicists from RHC section are stationed at various facilities in order to function in an advisory capacity.

The mandate of the section is to provide safety guidelines in terms of (i) Personnel exposure (ii) Effluents discharged (iii) Radiological conditions in the plant (iv) precautions to be followed during Special Operations (v) Handling of Unusual occurrences and (vi) emergency preparedness of the plant site.

Radiological Surveillance of BARC facilities

Due to the concerted efforts of the health physicists, there was a considerable reduction in the collective and average dose to the occupational workers of the nuclear facilities. Various systems like laundry monitor, scrap monitor, vehicle monitor, hotspot identification system, iodine, tritium and Ar-41 monitors have been developed and deployed in operating facilities. A close watch is kept on the environmental releases from the operating facilities through state of the art real time monitoring systems

to ensure regulatory compliance. This has resulted in appreciable reduction in environmental discharges there by reducing the exposures to the public. The divisional staff members participate in the proceedings of the various safety committees where safety reviews of the ongoing activities as well as of the upcoming projects are undertaken. The RHC personnel are actively associated with emergency training programmes and play an important role in formation and deployment of response teams during emergency situations and major national events.

In addition to these, the staff members are also associated with HRD programmes of RSSD, HPD, HRDD, ROD, FRD and Regulatory activities of BSC at BARC.

During the year 2012, about 3750 persons (inclusive of contractors) were monitored for radiation exposure and the collective dose incurred was 1985 p-mSv for the entire BARC site. In addition to the routine activities, operational health physics related development work is carried out by the RHC staff members. The members were actively associated with studies related to XI and XII plan projects of the Division. Support was also extended to the R & D activities carried out by the various Divisions of BARC.

Special Monitoring Techniques & R & D activities

Shielding evaluation and radiation monitoring for 14 MeV neutron generator

The Purnima building houses the 2.5 MeV (D,D) & 14 MeV (D,T) neutron generators. Detailed knowledge of the radiation dose rates around the neutron generators are essential for ensuring adequate radiological protection of the personnel involved with the operation of neutron generators. Verification and validation of the shield adequacy was carried out to reduce the neutron and associated gamma dose rates to the stipulated dose limits in full occupancy areas. This was achieved by measuring the neutron and gamma doserates at various locations inside and outside the Neutron generator hall during different operational conditions both for 2.5MeV and 14 MeV neutrons and comparing with theoretical simulation.

Monte Carlo Simulations

Detailed simulation of neutron and gamma transport occurring in and around neutron generators was carried out by FLUKA code to calculate neutron/gamma dose rates. Neutron and gamma dose rates were computed by using the ambient dose equivalent factors based on ICRP-74 publication. Several Monte Carlo runs were carried out to simulate the experimental conditions involving different combinations of shield thickness for both 14 MeV and 2.5 MeV neutron sources. Each FLUKA run involved tracking of about 2.2×10^8 source neutron histories and the statistical errors of the Monte Carlo runs are less than 2%. Based on the computation, an additional concrete shield of thickness 60cm around the existing building structure was recommended to operate at neutron yields at 5×10^9 n/s and above. The same has been implemented.

Experimental Measurements

Neutron and gamma dose rate measurements were conducted inside and outside the neutron generator hall for various source neutron yields ranging from 1×10^7 to 1×10^9 n/s. Neutron dose rates were measured using BF3 proportional counter-rem meters and MGPI make (Model DMC-2000) neutron-gamma personnel dosimeters. Fig. 1 shows a schematic of the experimental arrangement of detector locations inside the hall. Gamma measurements were carried out using plastic scintillator based survey meters, high range GM based survey meters (teletectors) and pocket ion chambers. Dose rate measurements showed a good agreement (up to 20% deviation) with FLUKA simulations. This study has served in generating detailed radiological dose rate maps around 2.5 MeV and 14 MeV neutron generators for various operational source neutron yields and
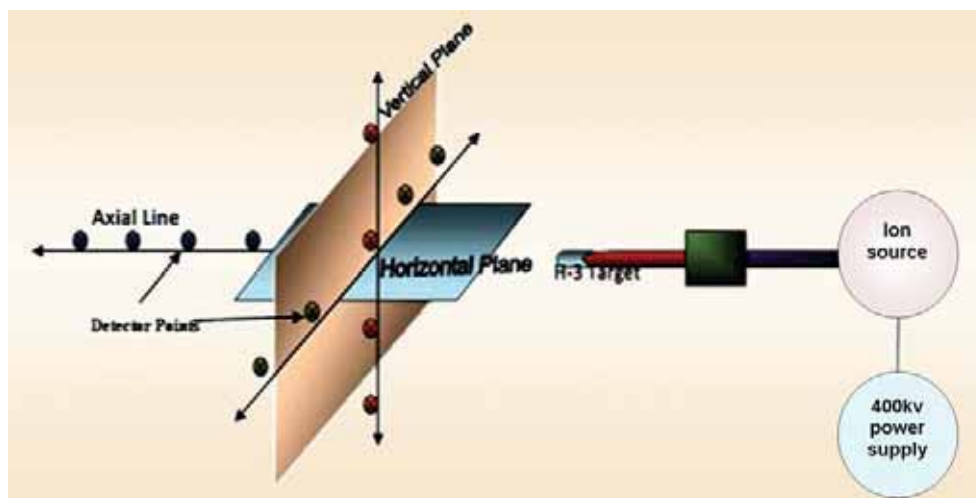

Fig. 1: Schematic of the detector locations for dose rate mapping in Purnima

also in benchmarking the Monte Carlo simulation methods adopted for dose rate evaluations and shield design of such facilities.

Development of Computed Tomography System for low level activity monitoring in MS drums

The system is aimed for estimating the presence of low levels of Cs-137 and Co-60 isotopes in standard 200L MS waste drums, which can qualify for clearance levels. Generally, the material and activity distribution in the waste drums are not uniform. An attenuation corrected spatial distribution of activity is to be estimated for each drum for accurate detection of low levels of activity. In the present method, the activity estimation is done in two stages. The self attenuation of drum is measured in the first stage using Transmission Computed
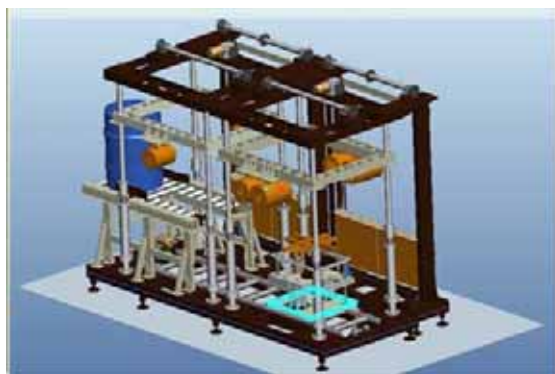

Fig. 2: Schematic sketch of Tomography based solid waste monitoring system.

Fig. 3: Final welding of the 3-axis manipulator at Workshop

Tomography (TCT). The TCT method gives spatial distribution of linear attenuation coefficient for the energy of interest. The second stage, Emission Computed Tomography (ECT) estimates the activity using the output of TCT for attenuation correction. As no assumptions regarding shape, size and location of material or activity are involved, the estimates will be more accurate than conventional methods. Fig.2 shows a schematic sketch of the waste drum monitoring station and Fig. 3 is the actual photograph of the 3-axis mechanical manipulator employed for the waste assay.

Transmission Computed Tomography (TCT)

The drum is considered to be consisting of horizontal layers. Each layer is individually scanned. The horizontal cross-section of drum is assumed to consist of a grid of square cells, each cell having a uniform μ value. A collimated beam of gamma radiation from a standard source is passed through this drum at different angles. The transmitted gamma flux reflects the total attenuation in the path of gamma ray. The total attenuation can be expressed as a sum of attenuation due to individual cells falling in the ray path. When several such rays are taken, a system of linear equations is obtained which can be represented in a matrix form. The solution to the system of linear equations gives the spatial distribution of μ values for the given energy.

Emission Computed Tomography (ECT)

A detector capable of energy resolution, (NaI(Tl)) is used to measure the activity of drum at different angles. The detector is shielded partially and is exposed to only a small portion of the drum. The activity in the exposed region can be related to counts registered by detector, corrected by μ values for the region obtained from TCT. Again, several measurements making a system of linear equations, when solved will give spatial distribution of activity corrected for self attenuation.

Development of a prototype System

A mathematical model is developed which implements TCT and ECT for given size of drum.

The mathematical model and reconstruction algorithm used for TCT stage are tested by physical experiments. A 3x manipulator for handling the drums was fabricated by Ms. Symec Engineers, MIDC, Turbhe. The system is fully automated. Different movements required by the drum and the detectors are controlled by SCADA routines which is integrated with a user written Central Control Program. A Central Control Program developed at RSSD facilitates to obtain inputs and controls the Hardware (3x manipulator) and the counting electronics (USB MCAs connected to the NaI detectors). The radiation measurement data obtained is analysed by the Tomography Reconstruction Algorithms for the estimation of final activity. Benchmarking/validation experiments with known sources after installation of system being planned at CIRUS reactor are to be conducted for successful demonstration of the system.

Tracer experiments in Mumbai Harbour Bay to study the transport of radioactive liquid waste discharge from Effluent Treatment Plant (ETP)

Effluent Treatment Plant, Trombay discharges low-level radioactive waste generated at Trombay site, in the Mumbai Harbour Bay from the discharge point located near the CIRUS Jetty in a controlled way after appropriate dilution. For radiological impact assessment for low-level liquid waste discharges to the Mumbai Harbour Bay from Effluent Treatment Plant (ETP), generation of various hydrological parameters that govern the transport of radioactivity in the Mumbai Harbour Bay is important. The hydrological parameters include study of the tidal current, bathymetry, dilution factor and hydrodynamic dispersion coefficient of the bay. For this purpose, a MoU has been signed to carry out this study with the help of the National Institute of Oceanography (NIO), Goa.

The dilution factor and hydrodynamic dispersion co-efficient is estimated using tracer technique. In this study, Br-82 radio tracer was used to estimate these parameters. In collaboration with Isotope Hydrology
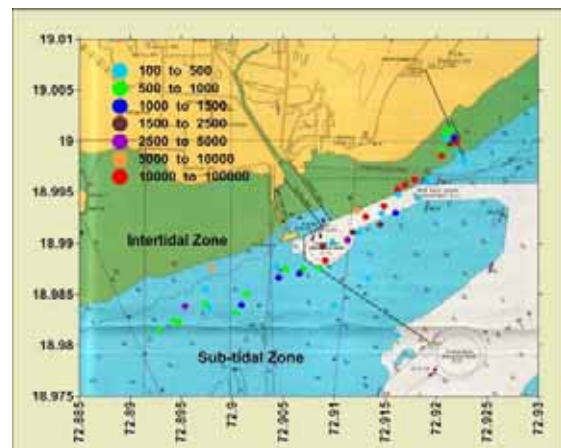

Fig. 4: Tracer flow pattern during ebb tide

Section, Isotope Application Division, two tracer experiments were conducted, one during ebb tide and other during flood tide. Br-82 radioactive source was injected in Mumbai Harbour Bay through discharge line of Effluent Treatment Plant (ETP), WMFT. In the first experiment, tracer was injected at full flood and in the second experiment, tracer was injected at full ebb and in both cases, movement of activity was tracked. The preliminary results of the experiment are presented in Figs. 4 and 5. In these figures the circular colored bullets depict count rate per minutes (CPM) of the gamma detector used to track the tracer movement. Fig.4 shows the tracer movement pattern during the ebb tide (when water flow back to sea) and Fig.5 shows tracer movement pattern during flood tide.
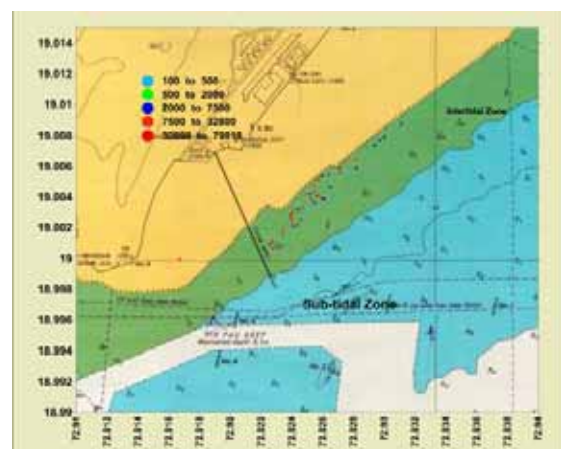

Fig. 5: Tracer flow pattern during flood tide

It can be observed, as expected, from Fig. 4 that during the ebb tide condition the migration of tracer is towards sea through sub-tidal zone. However during flood condition the tracer moves towards Thane creek parallel to shore line through intertidal zone (Fig. 5). The experimental findings indicate that for larger dilution of the radioactivity in the Mumbai Harbour Bay, effluent should be discharged during the start of the ebb tide as the effluent moves through sub-tidal zone. However, for discharges during flood tide, radioactivity will move mostly in inter-tidal zone where water depth is very low compared to sub-tidal zone thereby giving lesser dilution.

Radiological Safety Studies of Thorium Fuel Cycle

External Hazards

Radiological safety evaluation methods and systems were developed to augment the requirements of the Power Reactor Thorium Reprocessing Facility (PRTRF)[1-3]. Thorium oxide rods irradiated at PHWRs contain actinides like ^{232}U, ^{233}U and fission products. ^{228}Th, the daughter of ^{232}U has a alpha-decay half life of 1.9116 ± 0.0016 y and has a chain of daughter products of which ^{220}Rn (thoron), ^{208}Tl and ^{212}Bi are of major radiological concern. ^{208}Tl and ^{212}B are hard gamma emitters contributing to external exposure hazards in the thorium fuel cycle operations. The radiological aspects of handling fresh 54 pin composite cluster of the AHWR fuel were studied. The radial contact dose rates on the fresh AHWR fuel cluster is found to be 750 mSv/h, 3 years after fabrication.

Internal Hazards

^{220}Rn is a noble gas with a half life of 55.6 ± 0.1 sec, which contributes to inhalation exposure hazards in thorium fuel cycle. Regulatory requirements for thorium fuel cycle demand measurement of ^{220}Rn (Thoron) in the workplace and stack exhaust towards evaluation of internal exposures due to inhalation of the progeny of Thoron gas. ^{220}Rn occurs in the Thorium series in nature

and in the thorium fuel cycle, the gas is being continuously generated at higher than natural rates by the decay of ^{224}Ra that occurs in the decay chain of ^{228}Th.

Development of thoron monitor

A method has been developed to estimate the air-borne activity concentration of ^{220}Rn progeny in the workplace environs and in the gaseous effluent exhaust points based on gamma spectrometry using scintillation detectors. Air borne thoron is estimated by directly measuring the ^{208}Tl and other gamma emitters present in the chamber air after correcting for decay and build up of thoron daughters both due to air flow and radioactive decay phenomena. Pulse height distribution of simulated gamma spectrum corresponding to uniform distribution of ^{220}Rn activity inside the air-flow chamber and

Fig. 6: Thoron sampling chamber

calculated values of detector sensitivity and efficiency are estimated. Scintillation materials NaI(Tl), LaBr3 and BGO were tested for full energy peak area response using Monte Carlo simulation techniques. The system sensitivity works out to 0.08 cps per Thoron Working Level at thoron daughter product equilibrium, when one uses a 30 liter airflow chamber volume system without an inlet filter and 4"x6" NaI (Tl) crystal. For typical composite gamma photon energy spectrum from thoron daughters, LaBr3 and BGO are found to be 4 - 6 times more

sensitive than NaI (Tl), given the same active scintillator volumes. Fig.6 shows the photograph of thoron monitoring system.

Radiation Monitoring Instruments for PRTRF

In PRTRF, 2.6 MeV gamma ray photons are expected to be emitted from [208]Tl (daughter product of [228]Th). Based on the radiological shielding analysis of the facility, high energy gamma photons from [208]Tl arising from ppm levels of [232]U would dominate the spectrum in the final reconversion stages where the [233]U product is produced. Wide Range Gamma area employing appropriately compensated GM counters having linear energy response for gamma energies up to 3 MeV are found suitable for continuous dose rate measurements. For external radiation survey purposes, commercially available teletectors model AD-5 may be used. This model has linear response for photons up to 3 MeV. The criticality monitors need to be installed in cells/reconversion lab areas where gamma dose rates are less than 10 R/h. If the ambient gamma dose rates are much higher than 10 R/h, in order to avoid non-genuine alarms from the criticality point of view, the detector need to be shielded appropriately, such that the actual criticality incidents do not go undetected.

Design and fabrication of cryogenic gas chromatograph for rare gas separation

Measurement of low level krypton has many strategic and environmental applications. Enrichment and purification of krypton from air samples requires specially prepared gas handling

Fig. 7: Photograph of chromotography system for rare gas seperation

equipment which is not commercially available. A flow sheet is designed and the equipment is fabricated for this purpose and the performance of the assembly was tested with respect to leak tightness and detector response. In order to do trial runs on the integrated system, a gas mixing system is under design for preparing krypton containing mixture of predetermined composition.

Design criteria: Cryogenic Separation system

This system (Fig. 7) is designed to handle, 1-2 m³ of air and separate pure krypton gas from the mixture using multiple adsorption- desorption cycle within a time frame of 6-8 hours. The system is made of ¼" SS lines with adsorbent as charcoal and consists of four stainless steel columns successively reducing in size (from 500 cc to 20 cc) in order to achieve sufficient enrichment of krypton for further purification in analytical GC.

From column -1 onwards, the effluent gas is passing through a high volume thermistor detector (Gow Mac make) to detect the change in conductivity of the effluent. The effluent from one column can be switched to the next column or to the vent depending on the composition of the gases coming out. Elution from each column is achieved using successively increasing the column temperature using suitable temperature bath. Each adsorption-desorption cycle is expected to give more than 99% enrichment for krypton with respect to other major components of air. This system is designed to deliver $\sim 10^6$ times enrichment for krypton while subjecting the gas to three adsorption-desorption cycle. Leak tightness of the system and response of thermistor detectors to changing gas composition were tested and found satisfactory.

Analytical GC

Output from the last column of the enrichment system is fed to an online analytical GC, currently using 2 mL sampling loop (variable as per requirement in future) and a TCD detector. An 8 m long molecular sieve 5A column is procured for
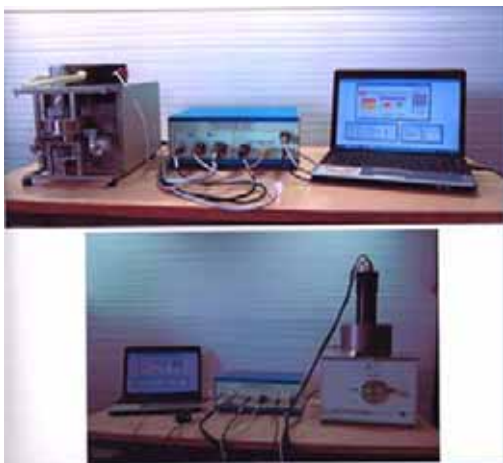
Fig. 8: Online stack monitor

achieving the desired separation. The design and fabrication of rare gas separation equipment is complete in all respect.

Fig. 9: Multiple alpha counting system

Design and Development of radiological monitoring systems at Radiological labs.

Online Stack Monitor

An online stack monitoring system (Fig 8) for radiological laboratories is designed for continuous

Fig.10: Online spot air sampler

monitoring of the radionuclides before releasing through stack to ensure that the activity discharged is within the authorized limit. The system uses techniques of alpha and gamma spectrometry. The efficiency of the alpha channel and gamma channel were found to be 10.10% and 9.57% respectively.

Multiple alpha counting system

A multiple alpha / beta counting system was designed and fabricated (Fig.9). It has arrangements for loading 10 samples in slots in order, get counted in a time programmed manner with results displayed and records maintained in PC. This automated design helped in reduction of man-hour consumption in counting and recording of the results.

Online spot air sampler

This is designed and fabricated to have in-situ measurement of alpha air activity. This device (Fig.10) contains a high volume pump, sample carousel to contain 4 centripeter sample heads and an alpha counting set up with necessary micro control programming for automation.

Radiological Surveillance during decommissioning of APSARA reactor

The first Indian research reactor, APSARA was utilized for various R & D programmes from 1956 till its

shutdown in 2009. The biological shield of the reactor developed residual activity due to neutron irradiation during the operation of the reactor. Dose rate mapping and in-situ gamma spectrometry
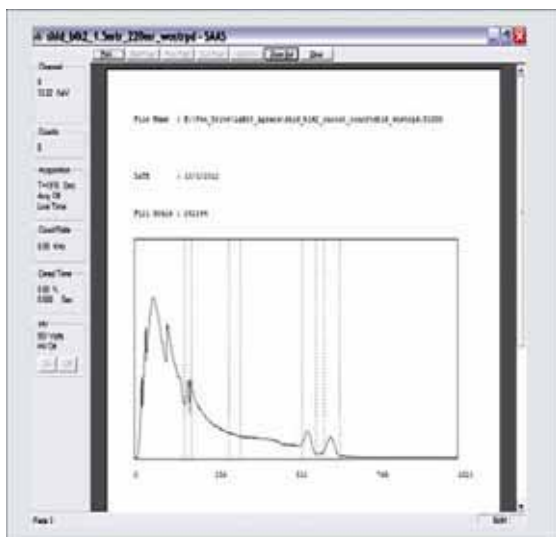

Fig. 11: *In-situ* gamma spectrum acquired using LaBr3 system in Apsara shield cubicle

(Fig. 11) of concrete structures of the reactor pool were carried out[4-5]. Based on the dose rate maps, representative concrete samples were collected from various locations and subjected to high resolution gamma spectrometry analysis. ^{60}Co and ^{152}Eu were found to be the dominant gamma emitting radionuclides in most of the locations. ^{133}Ba was also found in some of the concrete structures. Separation of ^{3}H from concrete was achieved using an acid digestion method and beta activity measured

using Liquid scintillation counting. Characterization of radioactivity in concrete is important for volume reduction of radioactive waste during decommissioning.

Acknowledgements

References

1. 'Assessment of Radiological Safety in Irradiated Thorium Fuel Handling Operations' P. Srinivasan, P. C. Gupta, D. N. Sharma, H. S. Kushwaha, proc of IRPA 12, Argentina, Oct 2008.

2. 'Assessment of thoron dose from dismantling of thoria dissolver in the ^{233}U pilot plant,' S. Priya., R. K. Gopalakrishnan, P. Srinivasan & M.G. Shinde, IARP conf., Jodhpur, Nov 2008.

3. 'Preliminary radiological safety assessment for decommissioning of thoria dissolver of the ^{233}U pilot plant, Trombay", S, Priya, P. Srinivasan and R K, Gopalakrishnan, Radiation Protection and Dosimetry, RPD-10-0387, March 2011

4. "Gamma dose rate mapping of APSARA structural components for decommissioning", Ignatious Jackson, P. Srinivasan, M. S. Belhe, V. S. Jayaram, S. N. Wankhede, Shibu Thomas and S. K. Prasad, 30th IARP Conference, IARPNC2012, Mangalore, March

5. A.Jassens, J.Buysse, F. Raes and H.Vanmarcke, *Nucl. Instr. Meth. Phys. Res.* B 17, 564 (1986).

27th Training Course on "Basic Radiological Safety and Regulatory Measures for Nuclear Facilities" : A Report

The BARC Safety Council Secretariat (BSCS) conducts series of short term training courses on "Basic Radiological Safety and Regulatory Measures for Nuclear Facilities" for the staff members of BARC to impart general awareness on basic radiological, industrial safety aspects and regulatory requirements. In this series BSC Secretariat conducted the 27th Training Course during May 27-30, 2013.

The training course was organized by Shri C.L.R. Yadav, BSCS and his team. About 60 participants up to the grade of SO/D from nine groups of BARC viz. MG, BMG, ChEG, CTG, E & IG, DM & AG, ESG, RD & DG and RPG attended the course. The training programme was carried out by way of classroom lectures, demonstrations and visits to

Emergency Response Centre and Dhruva Reactor. Faculty members were specialists with many years of experience from BSCS, HPD, RSSD, RP & AD, MD, IHSS and Fire Services Section. The training programme covered various aspects of safety including topics such as radiation protection programme in nuclear fuel cycle facilities, dosimetery and dose control, environmental radiation monitoring around nuclear facilities, occupational health care and management of internal contamination, preparedness and response for nuclear and radiological emergencies, biological effects of radiation and safety framework for BARC, safety culture.

Dignitaries, Dr. A.K. Ghosh, former Director, HS & EG, Dr. D.N. Sharma, Director, HS &EG and Shri Jose Joseph, Head, BSCS, invitees and participants after valedictory function of 27th Training Course on "BASIC RADIOLOGICAL SAFETY AND REGULATORY MEASURES FOR NUCLEAR FACILITIES"

"National Fire Service Week"- 2013

14th April is observed as National Fire Service Day. On this day in the year 1944, fire service personnel displayed exemplary courage and devotion to duty as they fought the major devastating fire that had erupted following an explosion on a Ship S.S. Fort Stikine berthed at the docks of Mumbai Port Trust. Many fire fighters lost their lives, leaving behind their names etched in the minds of mumbaites forever.

Several programmes were organized by the Fire Service Section, BARC during the Fire Service Week April 14 to 20, 2013 to create fire safety awareness among the employees in BARC, Trombay and residencies of Anushaktinagar.

On behalf of BARC, Shri P.B. Sarang, Station Officer placed a wreath on 14.4.2013 at the memorials erected on the grounds of Mumbai Port Trust and at the headquarters of Mumbai Fire Brigade, Byculla. A film on "Preventing Accident in the Home" was screened through cable network at Anushaktinagar on15th April. On the 16th, two crews from BARC Fire Service Section participated in the Tactical Medley Drill Competition organized by the Govt. of Maharashtra at Cross Maidan, Dhobi Talao, Mumbai. 18 teams belonging to various organizations viz. Mumbai Fire Brigade, BARC, Mumbai Port Trust, Maharashtra Industrial Development Corporation, Naval Dockyard, State Fire Academy, Thane Fire Brigade, Pune Fire Brigade, MSEB etc. participated in the competition. BARC team "B" received the First Consolation Prize and in the individual Ladder Drill competition the Second Prize. Shri Sekhar Basu, Director, BARC was offered a pin flag to inaugurate the fire service week and to start the fund raising campaign. "Fire Investigation" on fire safety was arranged for BARC officials at the Central Complex Auditorium. On 18.04.2013 a

Demonstration of Live Fire Fighting Operation

programme on Fire Fighting Equipment Exhibition with live fire fighting and rescue demonstration was organized at the AERB premises. Shri A.K. Tandle, Chief Fire Officer, BARC, briefed the audience about observance of fire service week, its importance and various programmes like rescue from high elevation, fire drill competition at State and Industrial level for fire professionals, fire safety awareness programme for BARC employees and residents of Anushaktingar. On 19th April, a programme on fire fighting equipment exhibition with live fire fighting and rescue demonstration was also organized at RUMP / UED. On 20th April, a prize distribution function was arranged at the Fire Station, BARC for winners of various competitions conducted among BARC fire service personnel. Shri K.T.Shenoy, Head, ChED and Shri S. Soundarajan, Head IHSS distributed the prizes to the winners of competition. This year Rs.27509 /- only were collected as cash donations during Fire Service Week Observance 2013. The Fire Service Week culminated with a ceremonial parade at Cross Maidan, Dhobi Talao, Mumbai in which BARC's Fire Service personnel contingent participated with Emergency Rescue Tender and equipment. Honorable Shri J.K. Sinha, Member, National Disaster Management Cell chaired the concluding function.

BRNS Theme meeting on Utilization of Accelerators: a report

The BRNS Theme meeting on Utilization of Accelerators was held on June 6, 2013 at the Electron Beam Centre, Navi Mumbai. The main aim of this meeting was to enhance the utilization of the 2 accelerators at EBC, viz. 10 MeV RF Linac and 3 MeV DC Accelerator.

A total of 182 participants registered for the theme meeting. This included 120 participants from BARC, 25 from Academic institutions, 15 from Industry and 22 from DAE & other Government units. Technical sessions included 10 invited talks and 10 contributory papers. Invited talks were presented by eminent specialists in their field of research on the topics pertinent to the theme of the meeting. The capabilities of the 10 MeV RF Linac and the 3 MeV DC Accelerator were highlighted. The advantages of electron-beam processing and the use of EBC accelerators for various applications including food preservation, medical sterilization, photofission experiments and material modification, were presented. The importance of safety issues in the operation of electron accelerators was also brought out. The proposal to use the 10 MeV RF Linac as Photon Source for Study of Nuclear Resonance Fluorescence held the potential to contribute greatly to the work of researchers in the field.

Spreading awareness about EB irradiation was another area which required great emphasis. It was felt that quarterly/half-yearly bulletins about EBC should be published and made available on a wide platform to spread information on the use of EB irradiation. Public media could also be used for this purpose. It was pointed out that projects for utilization of EBC accelerators could be undertaken through the AKRUTI framework of BARC. Development of low-cost EB accelerators suitable for rural India could also be planned.

In conclusion, the main emphasis at this juncture was the utilization of EBC accelerators for standardization of radiation processing applications and creating a hub for EB irradiation.

BARC Scientists Honoured

Name of the Scientist	:	**Dr. J.P. Mittal**
Affiliation	:	M.N. Saha Distinguished Fellow
Award	:	CRSI Gold medal for Life -time Achievement in Chemical Research
To be presented at	:	16 th National Symposium in Chemistry (NSC-16) to be held at the Indian Institute of Technology (IIT) Bombay, during February 6-9, 2014

Name of the Scientist	:	**Dr. Pitamber Singh**
Affiliation	:	Head, IADD, BARC
Award	:	**INS Outstanding Service Award for the year 2012** In High Technology Nuclear Related Areas

Name of the Scientist	:	**Shri Ram Kishan**
Affiliation	:	Associate Director, ESG, BARC
Award	:	INS Outstanding Service Award for the year 2012 Meritorious services in operating Plant or Engineering service